

Identification of Dihydrofuro[3,4-*d*]pyrimidine Derivatives as Novel HIV-1 Non-Nucleoside Reverse Transcriptase Inhibitors with Promising Antiviral Activities and Desirable Physicochemical Properties

Dongwei Kang,[†] Heng Zhang,[†] Zhao Wang,[†] Tong Zhao,[†] Tiziana Ginex,[‡] Francisco Javier Luque,[‡] Yang Yang,[§] Gaochan Wu,[†] Da Feng,[†] Fenju Wei,[†] Jian Zhang,[†] Erik De Clercq,^{||} Christophe Pannecouque,^{||} Chin Ho Chen,[⊥] Kuo-Hsiung Lee,^{#,v} N. Arul Murugan,[○] Thomas A. Steitz,[§] Peng Zhan,^{*,†} and Xinyong Liu^{*,†}

[†]Department of Medicinal Chemistry, Key Laboratory of Chemical Biology (Ministry of Education), School of Pharmaceutical Sciences, Shandong University, 44 West Culture Road, 250012 Jinan, Shandong, P. R. China

[‡]Department of Nutrition, Food Science and Gastronomy, Faculty of Pharmacy, Campus Torribera, Institute of Biomedicine (IBUB) and Institute of Theoretical and Computational Chemistry (IQTUCB), University of Barcelona, 08921 Santa Coloma de Gramenet, Spain

[§]Department of Molecular Biophysics and Biochemistry, Yale University, New Haven, Connecticut 06520-8114, United States

^{||}Laboratory of Virology and Chemotherapy, Rega Institute for Medical Research, KU Leuven, Herestraat 49 Postbus 1043 (09.A097), B-3000 Leuven, Belgium

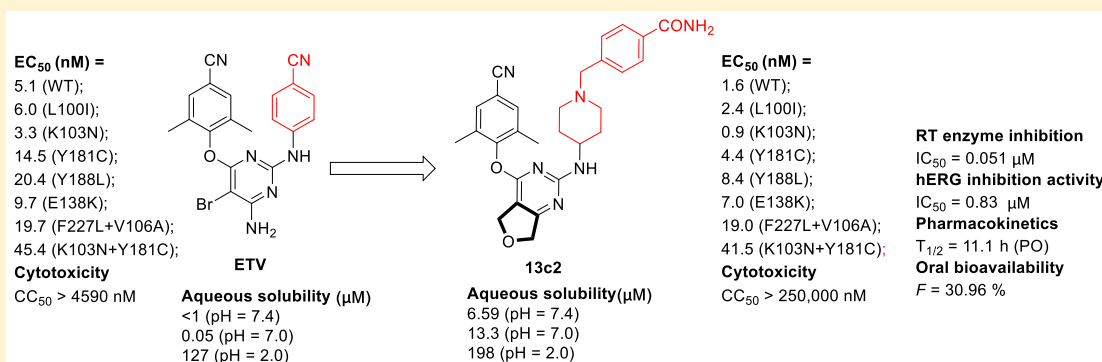
[⊥]Surgical Oncology Research Facility, Duke University Medical Center, Box 2926, Durham, North Carolina 27710, United States

[#]Natural Products Research Laboratories, Eshelman School of Pharmacy, University of North Carolina, Chapel Hill, North Carolina 27599, United States

^vChinese Medicine Research and Development Center, China Medical University and Hospital, Taichung 40402, Taiwan

[○]Department of Theoretical Chemistry and Biology, Royal Institute of Technology (KTH), AlbaNova University Center, S-106 91 Stockholm, Sweden

Supporting Information



ABSTRACT: To address drug resistance to HIV-1 non-nucleoside reverse transcriptase inhibitors (NNRTIs), a series of novel diarylpyrimidine (DAPY) derivatives targeting “tolerant region I” and “tolerant region II” of the NNRTIs binding pocket (NNIBP) were designed utilizing a structure-guided scaffold-hopping strategy. The dihydrofuro[3,4-*d*]pyrimidine derivatives **13c2** and **13c4** proved to be exceptionally potent against a wide range of HIV-1 strains carrying single NNRTI-resistant mutations (EC₅₀ = 0.9–8.4 nM), which were remarkably superior to that of etravirine (ETV). Meanwhile, both compounds exhibited comparable activities with ETV toward the virus with double mutations F227L+V106A and K103N+Y181C. Furthermore, the most active compound **13c2** showed favorable pharmacokinetic properties with an oral bioavailability of 30.96% and a half-life of 11.1 h, which suggested that **13c2** is worth further investigation as a novel NNRTI to circumvent drug resistance.

Received: October 24, 2018

Published: January 9, 2019

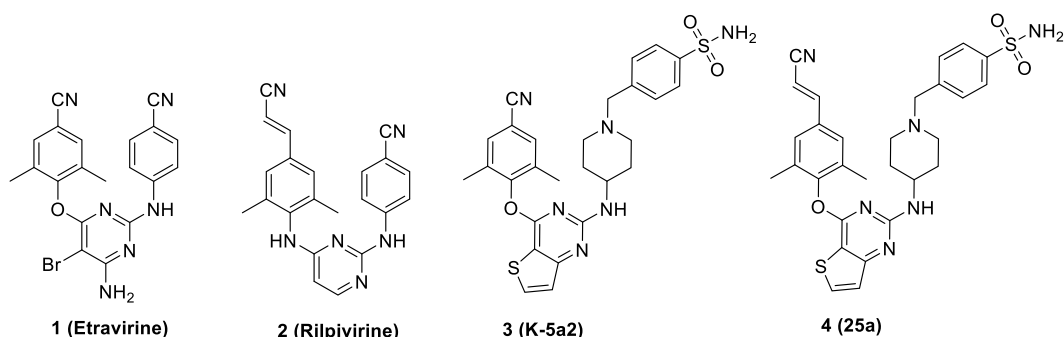


Figure 1. Chemical structures of U.S. FDA approved NNRTI drugs and our previously reported thiophene[3,2-*d*]pyrimidine leads **3** and **4**.

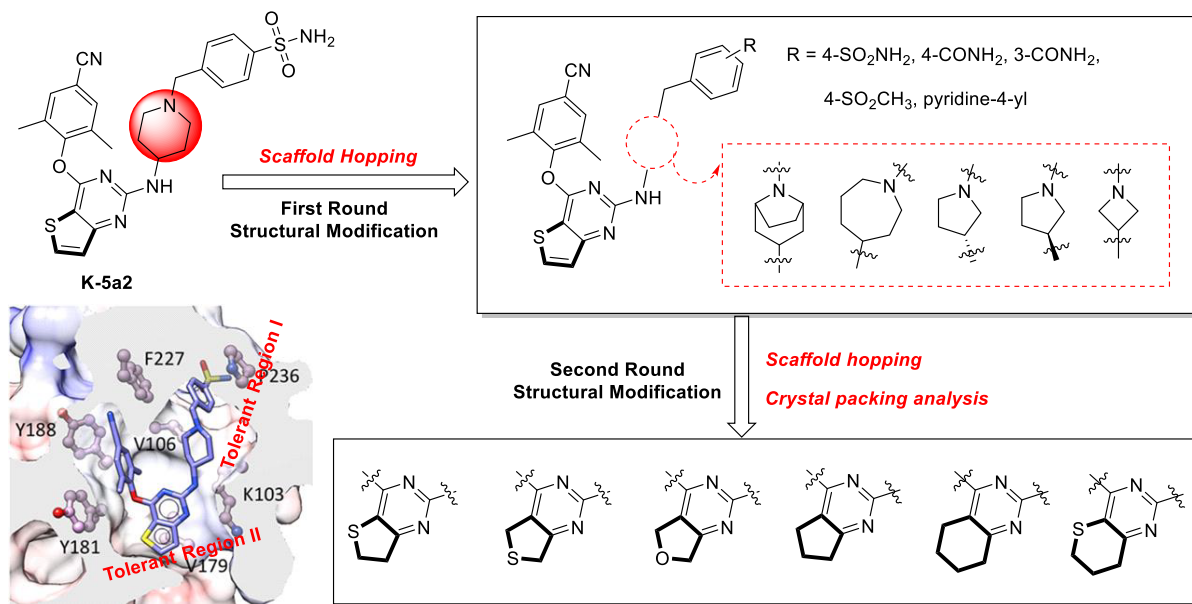


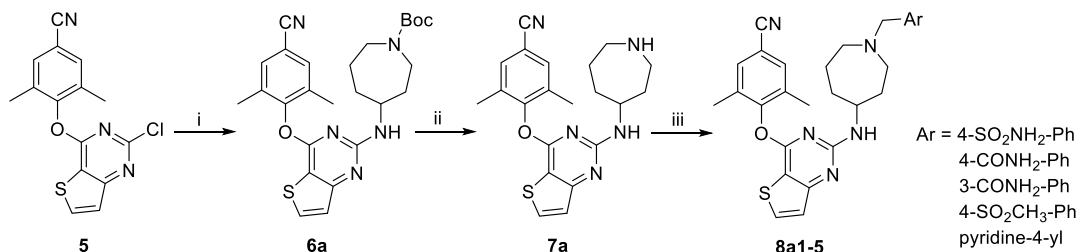
Figure 2. Further optimization of the piperidine linker and center thiophene[3,2-*d*]pyrimidine scaffold of the lead **3** (K-5a2) via scaffold hopping and crystal packing analysis.

INTRODUCTION

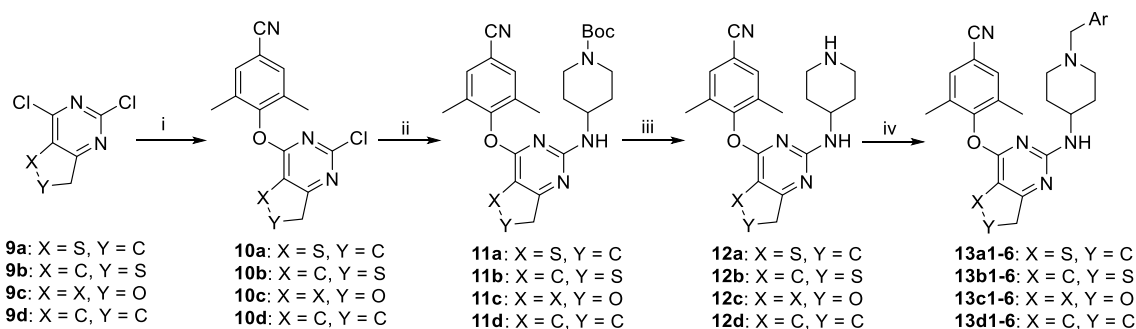
In the life cycle of HIV-1, reverse transcriptase (RT) is responsible for the reverse transcription of single-stranded RNA to double-stranded DNA and represents one of the most successful targets for the development of anti-HIV-1 therapeutics due to the well-characterized mechanisms of action and abundant structure information.^{1,2} RT inhibitors could be divided into nucleoside/nucleotide RT inhibitors (NRTIs/NtRTIs) and non-nucleoside RT inhibitors (NNRTIs).³ Especially, NNRTIs are widely used in highly active antiretroviral therapy (HAART) regimens, owing to their potent antiviral activity, high selectivity, and favorable pharmacokinetics. So far, six NNRTIs have been approved by U.S. Food and Drug Administration (FDA).⁴ Among them, nevirapine (NVP), delavirdine (DLV) and efavirenz (EFV) are the first-generation NNRTIs.⁵ However, toxicity and rapid emergence of drug resistance limited their clinical application. In particular, the K103N and Y181C mutations are prevalent in clinical HIV-1 isolates.^{6,7} Even in naïve patients, low frequencies of K103N and Y181C variants can lead to an increased risk of virologic failure.⁸ Diarylpyrimidine (DAPY) derivatives represent a promising class of second-generation NNRTIs, and two representative compounds etravirine (**1**, ETV) and rilpivirine (**2**, RPV) (see Figure 1) were approved by U.S. FDA in 2008 and

2011, respectively.⁵ Although they could effectively suppress most of the NNRTIs-resistant mutants selected by the treatment of the first-generation NNRTIs, drug resistance and adverse effects continue to emerge in patients receiving second-generation NNRTIs regimens.^{9,10} It underlines the demand to seek novel inhibitors with improved tolerability and resistance profiles.

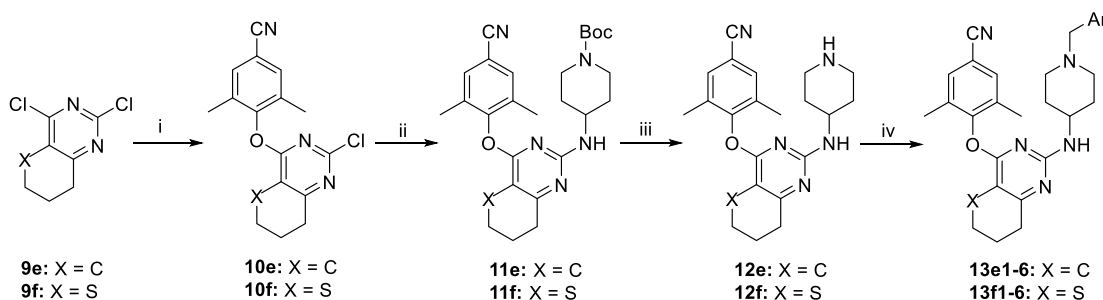
In the effort to discover structurally distinct, best-in-class NNRTIs, our group previously identified piperidine-substituted thiophene[3,2-*d*]pyrimidine derivatives **3** (K-5a2) and **4** (25a) (Figure 1), which showed extraordinarily potent anti-HIV-1 activities and improved antiresistance profiles compared with ETV.^{11–13} However, **3** exhibited weaker efficacy toward the particularly challenging double-mutation variant strain RES056 (K103N+Y181C) (EC₅₀ = 30.6 nM) compared with ETV (EC₅₀ = 17.0 nM). Although **4** achieved superior activity against RES056, it displayed a sharply increased cytotoxicity (CC₅₀ = 2.30 μM) than **3** (CC₅₀ > 227 μM). Apparently, the cyanovinyl group in the left wing of **4** accounts for the increased cytotoxicity considering that this chemical group may be sufficiently electrophilic to act as a “Michael acceptor”, resulting in potential covalent modification of nucleic acids, proteins, or other biological entities.¹⁴ Besides, lipophilic aromatic rings introduced to DAPY NNRTIs for better RT-binding affinities result in their poor aqueous solubility (the solubility of **3**, **4**, and ETV is

Scheme 1. Synthesis of 8a1–5^a

^aReagents and conditions: (i) *tert*-butyl 4-aminoazepane-1-carboxylate, DMF, K₂CO₃, 120 °C; (ii) TFA, DCM, rt; (iii) substituted benzyl chloride (or bromide) or 4-picolyl chloride hydrochloride, DMF, K₂CO₃, rt.

Scheme 2. Synthesis of 13a1–6, 13b1–6, 13c1–6, and 13d1–6^a

^aReagents and conditions: (i) 3,5-dimethyl-4-hydroxybenzonitrile, DMF, K₂CO₃, rt; (ii) *N*-(*tert*-butoxycarbonyl)-4-aminopiperidine, DMF, K₂CO₃, 120 °C; (iii) TFA, DCM, rt; (iv) substituted benzyl chloride (or bromide) or 4-picolyl chloride hydrochloride, DMF, K₂CO₃, rt.

Scheme 3. Synthesis of 13e1–6 and 13f1–6^a

^aReagents and conditions: (i) 3,5-dimethyl-4-hydroxybenzonitrile, DMF, K₂CO₃, rt; (ii) *N*-(*tert*-butoxycarbonyl)-4-aminopiperidine, DMF, K₂CO₃, 120 °C; (iii) TFA, DCM, rt; (iv) substituted benzyl chloride (or bromide) or 4-picolyl chloride hydrochloride, DMF, K₂CO₃, rt.

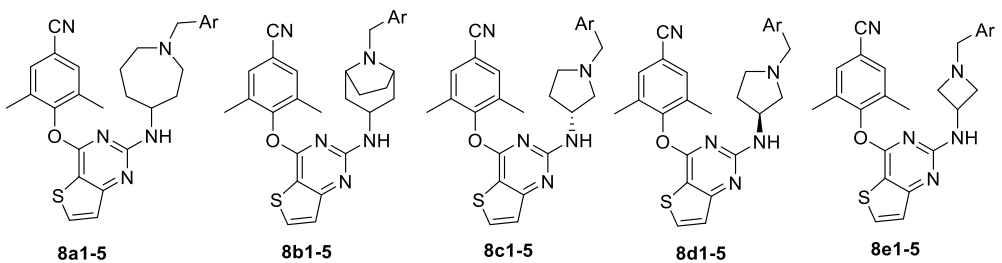
less than 1 μg/mL), likely due to the strong intermolecular π - π stacking interactions.¹⁵ Therefore, development of novel DAPY NNRTIs with enhanced potency and solubility is still highly necessary.

Our previous work on thiophene[3,2-*d*]pyrimidine DAPY inhibitors explored the structure–activity relationships (SARs) of the “tolerant region I” of NNRTI binding pocket (NNIBP) (Figure 2) and identified that aryl groups with multiple hydrogen bond donors or acceptors were preferred.¹¹ As an extension of the previous work on the scaffold of thiophene[3,2-*d*]pyrimidine, in this study we have kept the “privileged structure” of 3 unchanged, and explored elaborated structural modifications of the piperidine linker utilizing scaffold hopping strategy. Preliminary results prove that the piperidine linker plays a critical role in maintaining potent antiviral activities.

On the other hand, subsequent structural optimization has been focused on the center core of the lead guided by scaffold hopping and crystal packing analysis. In particular, the

thiophene[3,2-*d*]pyrimidine platform has been replaced by a set of six alicyclic-fused pyrimidine rings (Figure 2) with the hope that the additional alicyclic rings could change the crystal packing of the original aromatic ring structure and disrupt the possible intermolecular π - π stacking interactions, thus decreasing the lattice energy and improving the solubility.^{16,17} In addition, the exposed oxygen atom of dihydrofuro[3,4-*d*]pyrimidine is able to develop additional hydrogen bond interactions with amino acid residues in the NNIBP as a hydrogen bond receptor, which could contribute to improve the resistance profiles of compounds. Overall, the combination of those structural modification has led to dihydrofuro[3,4-*d*]pyrimidine derivatives as novel HIV-1 NNRTIs, which demonstrated not only significantly improved drug resistance profiles but also enhanced solubility and bioavailability.

Table 1. Anti-HIV-1 Activity and Cytotoxicity of 8a1–5, 8b1–5, 8c1–5, 8d1–5, and 8e1–5



| compd | Ar | NL4-3 | | |
|-----------|---------------------------------------|------------------------------------|------------------------------------|-----------------|
| | | EC ₅₀ (nM) ^a | CC ₅₀ (nM) ^b | SI ^c |
| 8a1 | 4-SO ₂ NH ₂ -Ph | 2.20 ± 0.67 | >222 | >100 |
| 8a2 | 4-CONH ₂ -Ph | >237 | >237 | X1 ^d |
| 8a3 | 3-CONH ₂ -Ph | 10.3 ± 5.05 | >237 | 23 |
| 8a4 | 4-SO ₂ CH ₃ -Ph | 9.98 ± 4.16 | >222 | 22 |
| 8a5 | pyridine-4-yl | 31.7 ± 11.0 | >257 | 8 |
| 8b1 | 4-SO ₂ NH ₂ -Ph | >217 | >217 | X1 ^d |
| 8b2 | 4-CONH ₂ -Ph | >232 | >232 | X1 ^d |
| 8b3 | 3-CONH ₂ -Ph | >232 | >232 | X1 ^d |
| 8b4 | 4-SO ₂ CH ₃ -Ph | >217 | >217 | X1 ^d |
| 8b5 | pyridine-4-yl | >251 | >251 | X1 ^d |
| 8c1 | 4-SO ₂ NH ₂ -Ph | 8.69 ± 2.74 | >233 | 26 |
| 8c2 | 4-CONH ₂ -Ph | 10.4 ± 2.70 | >250 | 24 |
| 8c3 | 3-CONH ₂ -Ph | 41.3 ± 14.4 | >250 | 6 |
| 8c4 | 4-SO ₂ CH ₃ -Ph | 13.9 ± 4.81 | >234 | 16 |
| 8c5 | pyridine-4-yl | 16.0 ± 4.24 | >273 | 17 |
| 8d1 | 4-SO ₂ NH ₂ -Ph | 104 ± 36.8 | >233 | 2.2 |
| 8d2 | 4-CONH ₂ -Ph | 55.7 ± 16.6 | >250 | 4.5 |
| 8d3 | 3-CONH ₂ -Ph | >250 | >250 | X1 ^d |
| 8d4 | 4-SO ₂ CH ₃ -Ph | 50.7 ± 12.8 | >234 | 4.6 |
| 8d5 | pyridine-4-yl | 16.7 ± 4.88 | >273 | 16 |
| 8e1 | 4-SO ₂ NH ₂ -Ph | 4.53 ± 1.30 | >240 | 53 |
| 8e2 | 4-CONH ₂ -Ph | 4.76 ± 1.50 | >257 | 54 |
| 8e3 | 3-CONH ₂ -Ph | 8.95 ± 2.64 | >257 | 29 |
| 8e4 | 4-SO ₂ CH ₃ -Ph | 207 ± 48.6 | >240 | 1.1 |
| 8e5 | pyridine-4-yl-Ph | 2.21 ± 0.61 | >282 | 128 |
| K-5a2 (3) | | 1.16 ± 0.43 | >227 | 196 |

^aEC₅₀: concentration of compound that causes 50% inhibition of viral infection and determined in at least triplicate against HIV-1 virus in TZM-bl cell lines. NL4-3 is wild-type HIV-1 viral strain. ^bCC₅₀: concentration that is cytopathic to 50% of cells. The highest concentration of the tested compounds was 125 ng/mL. ^cSI: selectivity index, the ratio of CC₅₀/EC₅₀. ^dX1: X1 means a value of SI > 1 or SI ≤ 1.

CHEMISTRY

All derivatives were synthesized by well-established methods as described in our previous article.¹² Representative synthetic routes of the series 8 that modify the piperidine linker are illustrated in Scheme 1. The previously prepared intermediate 5 was reacted with *tert*-butyl 4-aminoazepane-1-carboxylate to afford 6a, which gave the key intermediate 7a after removal of the Boc protecting group. Nucleophilic addition of 7a with substituted benzyl chloride (or bromine) or 4-picoyl chloride hydrochloride afforded target compounds 8a1–5. In an analogous way, 8b1–5, 8c1–5, 8d1–5, and 8e1–5 were prepared (Scheme S1 in Supporting Information).

The synthetic routes of series 13a, 13b, 13c, 13d, 13e, and 13f were depicted in Schemes 2 and 3. 2,4-Dichloro-substituted pyrimidines 9a–f were selected as the starting materials and were reacted with 4-hydroxy-3,5-dimethylbenzonitrile by nucleophilic substitution to produce 10a–f. Then another successive nucleophilic addition of 4-(*tert*-butoxycarbonyl)-aminopiperidine with 10a–f generated intermediates 11a–f, which were converted to target compounds 13a1–6, 13b1–5,

13c1–6, 13d1–6, 13e1–6, and 13f1–5 followed by a similar procedure in Scheme 1.

RESULTS AND DISCUSSION

The target compounds 8a1–5, 8b1–5, 8c1–5, 8d1–5, and 8e1–5 were evaluated against wild-type (WT) HIV-1 (NL4-3) replication in TZM-bl cell lines, and compounds 13a1–6, 13b1–5, 13c1–6, 13d1–6, 13e1–6, and 13f1–5 were evaluated against WT HIV-1 (IIIB), NNRTI-resistant strain K103N+Y181C (RES056), and a HIV-2 strain (ROD) in the MT4 cell line. Etravirine (ETV) was selected as control drug. The values of EC₅₀ (anti-HIV potency), CC₅₀ (cytotoxicity), SI (selectivity index, CC₅₀/EC₅₀ ratio) of the synthesized compounds are summarized in Tables 1–5. In addition, the RF (fold-resistance factor, EC₅₀ against mutant strains/EC₅₀ against WT strain) values of some potent compounds are shown in Table 5.

First, we assessed the anti-HIV-1 activities of the novel derivatives 8a1–5, 8b1–5, 8c1–5, 8d1–5, and 8e1–5 in which the piperidine linker of the lead 3 was replaced by nitrogen-

Table 2. Anti-HIV (IIIB, RES056, and ROD) Activity and Cytotoxicity of 13a1–6, 13b1–5, 13c1–6, and 13d1–6

| compd | Ar | EC ₅₀ (nM) ^a | | EC ₅₀ (μM) ^a | | SI ^c | |
|-------|---------------------------------------|------------------------------------|-------------|------------------------------------|------------------------------------|-----------------|--------|
| | | IIIB | RES056 | ROD | CC ₅₀ (μM) ^b | IIIB | RES056 |
| 13a1 | 4-SO ₂ NH ₂ -Ph | 4.3 ± 0.7 | 28.8 ± 1.2 | 6.55 ± 0.82 | 19.9 ± 10.1 | 4584 | 692 |
| 13a2 | 4-CONH ₂ -Ph | 4.8 | 43.6 ± 5.0 | >165 | 165 ± 36.9 | 34162 | 3804 |
| 13a3 | 4-SO ₂ CH ₃ -Ph | 5.9 ± 1.3 | 46.6 ± 7.8 | 13.5 ± 9.00 | 11.9 ± 5.57 | 2025 | 257 |
| 13a4 | pyridine-4-yl | 2.6 ± 1.0 | 46.0 ± 1.9 | 15.7 ± 12.2 | ≥106 | ≥40104 | ≥2305 |
| 13a5 | 4-NO ₂ -Ph | 8.0 ± 1.7 | 495 ± 1.3 | >6.18 | 6.18 ± 1.74 | 770 | 12 |
| 13a6 | 3-CONH ₂ -Ph | 27.7 ± 21.5 | 629 ± 64.5 | >223 | ≥223 | ≥8048 | ≥355 |
| 13b1 | 4-SO ₂ NH ₂ -Ph | 37.2 ± 26.6 | 734 ± 337.2 | ≥26.7 | 26.6 ± 1.96 | 715 | 36 |
| 13b2 | 4-SO ₂ Me-Ph | 3.8 ± 1.3 | 170 ± 32 | ≥22.7 | 45.3 ± 31.1 | 11690 | 259 |
| 13b3 | 4-NO ₂ -Ph | 11.5 ± 0.4 | 1143 ± 108 | >27.1 | 27.1 ± 2.55 | 2341 | 24 |
| 13b4 | 4-NH ₂ -Ph | 8.4 ± 2.8 | 704 ± 273 | 108 ± 53.3 | >256.9 | >30377 | >364 |
| 13b5 | 4-NHSO ₂ Me-Ph | 11.2 ± 0.6 | 5240 ± 1500 | >257 | >256.9 | >19670 | >42 |
| 13c1 | 4-SO ₂ NH ₂ -Ph | 2.8 ± 1.0 | 38.0 ± 7.5 | ≥8.37 | 27.5 ± 7.49 | 9518 | 725 |
| 13c2 | 4-CONH ₂ -Ph | 1.6 ± 0.4 | 41.5 ± 9.9 | 12.7 ± 0.72 | >250 | >156250 | >6039 |
| 13c3 | 4-SO ₂ CH ₃ -Ph | 1.9 ± 0.1 | 41.6 ± 4.9 | >27.0 | 31.3 ± 7.2 | 15946 | 752 |
| 13c4 | pyridine-4-yl | 2.3 ± 0.2 | 43.1 ± 1.2 | 5.12 ± 1.85 | 37.6 ± 11.0 | 15895 | 871 |
| 13c5 | 4-NO ₂ -Ph | 7.4 ± 0.9 | 511 ± 165 | >11.1 | ≥11.1 | ≥1497 | ≥22 |
| 13c6 | 3-CONH ₂ -Ph | 7.8 ± 3.4 | 1033 ± 51.1 | 209 ± 29.7 | >250 | >31780 | >243 |
| 13d1 | 4-SO ₂ NH ₂ -Ph | 1.1 ± 0.5 | 25.8 ± 1.19 | 58.3 ± 4.28 | >234 | >208333 | >9091 |
| 13d2 | 4-CONH ₂ -Ph | 6.1 ± 2.7 | 173 ± 110 | 139 ± 24.3 | >251 | >40984 | >1448 |
| 13d3 | 4-SO ₂ CH ₃ -Ph | 4.9 ± 0.8 | 187 ± 0.79 | 41.8 ± 5.76 | 7.45 ± 0.93 | 1495 | 40 |
| 13d4 | pyridine-4-yl | 1.8 ± 0.7 | 54.7 ± 6.22 | 138 ± 25.7 | >274 | >147059 | >5020 |
| 13d5 | 4-NO ₂ -Ph | 14.5 ± 3.6 | 941 ± 368 | >8.73 | 8.73 ± 3.53 | 599 | 9 |
| 13d6 | 3-CONH ₂ -Ph | 2.0 ± 0.5 | 26786 | >205 | 205 ± 1.13 | 124410 | 9 |
| ETV | | 5.1 ± 0.8 | 45.4 ± 15.5 | | >4.59 | >889 | >101 |

^aEC₅₀: concentration of compound required to achieve 50% protection of MT-4 cell cultures against HIV-1-induced cytopathic, as determined by the MTT method. ^bCC₅₀: concentration required to reduce the viability of mock-infected cell cultures by 50%, as determined by the MTT method. ^cSI: selectivity index, the ratio of CC₅₀/EC₅₀.

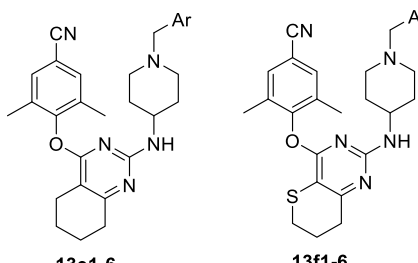
containing cyclic analogues (Table 1). Most derivatives in subseries-8a, subseries-8c, subseries-8d, and subseries-8e were active against WT HIV-1 strain with moderate to high potencies (EC₅₀ = 2.20–207 nM), while the compounds in subseries-8b displayed dramatically impaired anti-HIV potency even at the maximum tested concentration (1 μg/mL). Compounds in subseries-8e featuring an azetidine linker yielded the most active potency with EC₅₀ values ranging from 2.21 to 8.95 nM with an exception of 8e4 (EC₅₀ = 207 nM). Among these derivatives, 8a1 and 8e5 proved to be the most effective inhibitors (EC₅₀ = 2.20 and 2.21 nM, respectively), comparable to that of 3 (EC₅₀ = 1.16 nM).

The preliminary SARs indicated that the linker of the right wing affected the activity significantly. Comparison of the designed five linkers indicates that the piperidine linker in the lead 3 was crucial for the potent antiviral activities. Furthermore, this result revealed that the cytotoxicity was not directly related to the modification of the piperidine linker.

To design more potent NNRTIs with improved drug resistance profiles and optimal physicochemical properties, a scaffold-hopping approach was applied to the center core

(exploiting “tolerant region II”). The activities of five-membered ring fused pyrimidine derivatives 13a1–6, 13b1–5, 13c1–5, and 13d1–6, characterized by different scaffolds, are shown in Table 2. All the compounds displayed promising activity against WT HIV-1 with EC₅₀ values ranging from 1.6 to 37.2 nM. The compounds in subseries-13c and subseries-13d exhibited the most potent activity against WT HIV-1. Compounds 13c2, 13c3, 13d1, 13d4, and 13d6 turned out to be the most potent inhibitors, with EC₅₀ values ranging from 1.1 to 2.0 nM, being about 2.5- to 4.6-fold more potent than the reference drug ETV (EC₅₀ = 5.1 nM). In addition, 13a1, 13a2, 13a4, 13b2, 13c1, 13c4, and 13d3 also showed higher potency than ETV with EC₅₀ values of 2.3–4.9 nM. Importantly, these potent compounds exhibited extremely high SI values (SI > 10 000) except for 13a1 (SI = 4584) and 13c1 (SI = 9518). Moreover, 13a1–4 and 13c1–4 showed promising activity (EC₅₀ = 28.8–46.6 nM) against the double mutant strain RES056, being similar to or more potent than that of ETV (EC₅₀ = 45.4 nM). 13a1 was the most potent inhibitor with an EC₅₀ value of 28.8 nM, about 1.5-fold more potent than ETV. In addition, the results also suggest that some compounds exhibited micromole activity against

Table 3. Anti-HIV (IIIB, RES056, and ROD) Activity and Cytotoxicity of 13e1–6 and 13f1–6



| compd | Ar | EC ₅₀ (nM) | | EC ₅₀ (μM) | | SI | |
|-------|---------------------------------------|-----------------------|-------------|-----------------------|-----------------------|--------|--------|
| | | IIIB | RES056 | ROD | CC ₅₀ (μM) | IIIB | RES056 |
| 13e1 | 4-SO ₂ NH ₂ -Ph | 6.0 ± 2.3 | 667 ± 556 | >228 | >228 | >37879 | >342 |
| 13e2 | 4-CONH ₂ -Ph | 6.0 ± 2.0 | 291 ± 185 | >233 | >233 | >38709 | >799 |
| 13e3 | 4-SO ₂ CH ₃ -Ph | 8.0 ± 3.1 | 66.1 ± 4.52 | ≥163 | >266 | >33333 | >4032 |
| 13e4 | pyridine-4-yl | 8.6 ± 0.7 | 172 ± 20.2 | 21.7 ± 0.96 | 75.8 ± 45.1 | 8748 | 440 |
| 13e5 | 4-NO ₂ -Ph | 77.4 ± 46.5 | 6896 ± 1104 | >29.1 | 29.1 ± 7.19 | 376 | 4 |
| 13e6 | 3-CONH ₂ -Ph | 6.5 ± 3.3 | 3148 ± 315 | >158 | 158 ± 35.8 | 24415 | 50 |
| 13f1 | 4-SO ₂ NH ₂ -Ph | 2.7 ± 2.6 | 40.6 ± 6.7 | >148 | ≥148.2 | ≥54889 | ≥3650 |
| 13f2 | 4-CONH ₂ -Ph | 3.0 ± 2.8 | 93.0 ± 77.3 | >44.3 | ≥44.3 | >14767 | >476 |
| 13f3 | 4-SO ₂ CH ₃ -Ph | 3.9 ± 2.0 | 98.3 ± 59.6 | >3.40 | ≥3.4 | ≥872 | ≥34.6 |
| 13f4 | 4-NO ₂ -Ph | 8.6 ± 4.7 | 604 ± 83.9 | >4.00 | 4.0 ± 0.3 | 465 | 6.6 |
| 13f5 | 3-CONH ₂ -Ph | 5.1 ± 0.4 | 1049 ± 149 | >5.80 | 5.8 ± 3.7 | 1137 | 5.5 |
| ETV | | 5.1 ± 0.8 | 45.4 ± 15.5 | | >4.59 | >889 | >101 |

Table 4. Activity against Mutant HIV-1 Strains of 13a1-2, 13c1-4, 13d1 and 13f1

| compd | EC ₅₀ (nM) | | | | | |
|-------|-----------------------|------------|------------|-------------|-------------|-------------|
| | L100I | K103N | Y181C | Y188L | E138K | F227L+V106A |
| 13a1 | 5.8 ± 0.7 | 5.9 ± 0.1 | 8.0 ± 0.3 | 10.1 ± 0.7 | 12.8 ± 0.2 | 13.7 ± 0.6 |
| 13a2 | 15.2 ± 1.4 | 5.0 ± 1.0 | 8.4 ± 0.9 | 22.1 ± 0.55 | 15.3 ± 2.7 | 36.5 ± 1.0 |
| 13c1 | 3.0 ± 1.1 | 2.9 ± 0.5 | 5.4 ± 0.0 | 15.2 ± 0.3 | 7.9 ± 0.6 | 12.7 ± 7.6 |
| 13c2 | 2.4 ± 0.2 | 0.9 ± 0.1 | 4.4 ± 1.1 | 8.4 ± 3.6 | 7.0 ± 2.5 | 19.0 ± 2.2 |
| 13c3 | 3.4 ± 0.9 | 2.0 ± 1.0 | 4.9 ± 0.1 | 7.9 ± 0.9 | 7.8 ± 2.6 | 7.2 ± 0.1 |
| 13c4 | 4.1 ± 0.6 | 1.2 ± 0.1 | 4.9 ± 0.1 | 7.8 ± 1.5 | 6.2 ± 1.0 | 10.5 ± 0.6 |
| 13d1 | 5.9 ± 0.1 | 11.0 ± 8.7 | 14.2 ± 0.2 | 14.0 ± 3.9 | 42.3 ± 10.4 | 35.6 ± 8.4 |
| 13f1 | 12.9 ± 2.9 | 5.2 ± 1.4 | 10.4 ± 1.9 | 8.0 ± 2.0 | 8.5 ± 0.8 | 22.3 ± 4.8 |
| ETV | 6.0 ± 1.5 | 3.3 ± 0.6 | 14.5 ± 8.2 | 20.4 ± 8.6 | 9.7 ± 6.9 | 19.7 ± 7.3 |

Table 5. SI and RF Values of 13a1-2, 13c1-4, 13d1 and 13f1

| compd | SI (RF) ^a | | | | | |
|-------|----------------------|---------------|---------------|---------------|--------------|---------------|
| | L100I | K103N | Y181C | Y188L | E138K | F227L+V106A |
| 13a1 | 2880 (1.2) | 2835 (1.3) | 2071 (1.7) | 1645 (2.2) | 1298 (2.7) | 1220 (2.9) |
| 13a2 | 9576 (3.3) | 28912 (1.1) | 17281 (1.8) | 6594 (4.8) | 9515 (3.3) | 3999 (7.9) |
| 13c1 | 8941 (1.1) | 9220 (1.0) | 5087 (1.9) | 1810 (5.3) | 3471 (2.7) | 2270 (4.2) |
| 13c2 | >104167 (1.5) | >277778 (0.6) | >56818 (2.8) | >29762 (5.3) | >35714 (4.4) | >13158 (11.9) |
| 13c3 | 9050 (1.8) | 15221 (1.0) | 6318 (2.5) | 3940 (4.0) | 3986 (4.0) | 4349 (3.7) |
| 13c4 | 9035 (1.8) | 31212 (0.5) | 7630 (2.1) | 4769 (3.3) | 6023 (2.6) | 3576 (4.4) |
| 13d1 | >39683 (5.3) | >21186 (10) | >16447 (12.9) | >16667 (12.7) | >5543 (38.4) | >6579 (32.3) |
| 13f1 | ≥11488 (4.7) | ≥28500 (1.9) | ≥14250 (3.8) | ≥18525 (3.0) | ≥17435 (3.1) | ≥6645 (8.3) |
| ETV | >755 (1.1) | >1379 (0.6) | >315 (2.3) | >225 (3.3) | >471 (1.6) | >233 (3.2) |

^aRF is the ratio of EC₅₀(resistant viral strain)/EC₅₀(wild-type viral strain).

HIV-2 (ROD), such as **13a1** (EC₅₀ = 5.1 μM) and **13c4** (EC₅₀ = 5.1 μM), which could be considered as potential lead compounds for further optimization to find novel HIV-2 inhibitors with new mechanisms of action.

The activities of derivatives **13e1–6** and **13f1–5** bearing tetrahydroquinazoline and 7,8-dihydro-6H-thiopyrano[3,2-d]pyrimidine center cores, respectively, are summarized in Table

3. 13f1 (EC₅₀ = 2.7 nM) and **13f2** (EC₅₀ = 3.0 nM) exhibited prominent potency against WT HIV-1, comparable to that of ETV. Although most compounds of subseries **13e** showed single-digit activity toward WT HIV-1, their potencies against RES056 were inferior to that of ETV. Among them, the most effective inhibitor **13f1** (EC₅₀ = 40.6 nM) exhibited similar activity as ETV.

Table 6. Inhibitory Activity against WT HIV-1 RT

| compd | IC ₅₀ (μM) | compd | IC ₅₀ (μM) | compd | IC ₅₀ (μM) |
|-------|-----------------------|-------|-----------------------|-------|-----------------------|
| 13a1 | 0.074 ± 0.002 | 13b5 | 0.140 ± 0.013 | 13d4 | 0.073 ± 0.007 |
| 13a2 | 0.066 ± 0.005 | 13c1 | 0.109 ± 0.003 | 13d5 | 0.241 ± 0.009 |
| 13a3 | 0.130 ± 0.033 | 13c2 | 0.051 ± 0.001 | 13d6 | 0.241 ± 0.009 |
| 13a4 | 0.112 ± 0.023 | 13c3 | 0.077 ± 0.009 | 13e1 | 0.084 ± 0.015 |
| 13a5 | 0.175 ± 0.047 | 13c4 | 0.056 ± 0.003 | 13e2 | 0.051 ± 0.004 |
| 13a6 | 0.094 ± 0.009 | 13c5 | 0.092 ± 0.024 | 13e3 | 0.089 ± 0.011 |
| 13b1 | 0.410 ± 0.112 | 13c6 | 0.091 ± 0.007 | 13e4 | 0.072 ± 0.003 |
| 13b2 | 0.091 ± 0.027 | 13d1 | 0.091 ± 0.029 | 13e5 | 0.094 ± 0.004 |
| 13b3 | 0.129 ± 0.057 | 13d2 | 0.073 ± 0.015 | 13e6 | 0.101 ± 0.016 |
| 13b4 | 0.115 ± 0.008 | 13d3 | 0.157 ± 0.022 | ETV | 0.011 ± 0.000 |

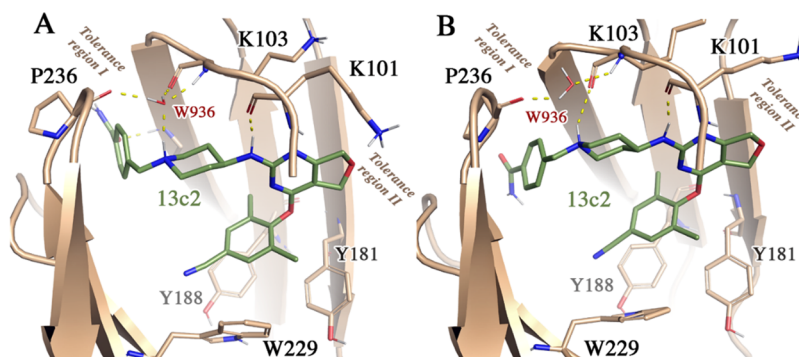


Figure 3. Initial (A) and final (B) binding mode for ligand 13c2 into the NNIBP (PDB code 6C0J). The displacement of the water molecule occurred during MD simulations, enabling the formation of a direct hydrogen bond between the backbone carbonyl oxygen of K103 and the protonated pyrimidine nitrogen.

Analysis of the SARs of these six subseries derivatives demonstrated that the hydrophilic substituents harboring hydrogen bond donors or acceptors (i.e., Ar = 4-SO₂NH₂-Ph, 4-SO₂CH₃-Ph, 4-CO₂NH₂-Ph, and pyridine-4-yl) were preferred. On the contrary, the hydrophobic substituents (i.e., Ar = 4-NO₂-Ph) were detrimental to its potency against WT HIV-1 and especially against mutated strains. 13a5, 13b3, 13c5, 13d5, 13e5, and 13f5 only exerted moderate activity with EC₅₀ values of 495, 1143, 511, 941, 6896, and 604 nM toward RES056, respectively. Pairwise comparison of the activities (compounds 13a1 vs 13a6, 13c1 vs 13c6, 13d1 vs 13d6, 13e1 vs 13e6, and 13f1 vs 13f5) confirmed the critical role of the *para*-substitution in improving the activity against RES056 over *meta*-substitution. Furthermore, the fused heterocycle on the pyrimidine was found to have a major influence on their anti-HIV-1 activity, especially against RES056. For instance, 13a1–4 (EC₅₀ = 28.8–46.6 nM) with dihydrothieno[3,2-*d*]pyrimidine and 13c1–4 (EC₅₀ = 38.0–43.1 nM) with dihydrofuro[3,4-*d*]pyrimidine scaffold exhibited prominent potency against RES056, while the activity of subseries 13b with dihydrothieno[3,4-*d*]pyrimidine scaffold considerably decreased (EC₅₀ = 170–5240 nM).

Subsequently, the efficacy of the compounds with potent activities toward WT and RES056 HIV-1 (13a1,2, 13c1–4, 13d1, and 13f1) were evaluated in MT-4 cells against mutant HIV-1 strains harboring single amino acid mutations L100I, K103N, Y181C, Y188L, E138K and double mutation F227L +V106A in the RT (Table 4 and Table 5). The results demonstrated that 5,7-dihydrofuro[3,4-*d*]pyrimidine derivatives 13c1–4 were potent inhibitors of the whole viral panel of NNRTI-resistant strains. Especially, 13c2 and 13c4 exhibited higher potency against K103N mutant strain than WT HIV-1 strain (RF = 0.6 and 0.5, respectively), with EC₅₀ values of 0.9 and 1.2 nM, about 2.7- and 3.6-fold lower than that of ETV

(EC₅₀ = 3.3 nM). In the case of L100I, Y181C, Y188L, and E138K, 13c2, 13c3, and 13c4 provided single-digit nanomolar activities (EC₅₀ = 0.9–8.4 nM), being superior to that of ETV. For F227L+V106A, 13c3 (EC₅₀ = 7.2 nM) showed the highest potency and was 2.7-fold more potent than ETV (EC₅₀ = 19.7 nM). Moreover, 13a1, 13c1, 13c2, and 13c4 also inhibited F227L+V106A (EC₅₀ = 13.7, 12.7, 19.0, and 10.5 nM) to a greater extent than ETV. However, dihydrothieno[3,2-*d*]pyrimidine derivative 13a2 and dihydrofuro[3,4-*d*]pyrimidine derivative 13d1 exhibited weaker efficacy toward most of the mutations compared with ETV. Specifically, 13d1 inhibited the two most prevalent single mutations K103N and E138K with much lower activity (EC₅₀ = 11.0 and 42.3 nM) and higher relative factor (RF) values (10 and 38.4) in comparison to ETV (EC₅₀ = 3.3 and 9.7 nM, RF = 0.6 and 1.6) (Table 5).

Some representative derivatives were further evaluated for their ability to inhibit recombinant WT HIV-1 RT enzyme to confirm the binding target (data shown in Table 6). Except for 13b1, 13d5, and 13d6, most compounds demonstrated high binding-affinity to WT HIV-1 RT (IC₅₀ = 0.051–0.175 μM). Generally, the derivatives with hydrophobic substituent and *meta*-substituent group have reduced inhibitory activities, exemplified by these pairwise comparisons: 13a1–4 vs 13a5, 13c1–4 vs 13c5,6, 13d1–4 vs 13d5,6, and 13e1–4 vs 13e5,6. Unexpectedly, the compounds containing 4-CONH₂-Ph substituent (13a2, 13b2, 13c2, 13d2, and 13e2) offered the highest RT inhibitory activities in each subseries, which were inconsistent with their anti-HIV-1 potency. This discrepancy, which has been reported in our previous articles, may be caused by the variations in the HIV-1 RT-substrate binding affinities and polymerase processivity on different nucleic acid templates.^{11,18} Nonetheless, these results suggest that the newly synthesized derivatives behave as typical NNRTIs.

Table 7. Physicochemical Parameters of 13a1 and 13c1–4

| compd | aqueous solubility ($\mu\text{g/mL}$) ^a | | | FaSSIF ^b | log <i>P</i> ^c | LE ^d | LLE ^e | LELP ^f |
|-------|--|--------|--------|---------------------|---------------------------|-----------------|------------------|-------------------|
| | pH 7.4 | pH 7.0 | pH 2.0 | | | | | |
| 13a1 | 2.54 | 8.26 | 192 | 10.0 | 3.73 | 0.30 | 4.63 | 12.4 |
| 13c1 | 5.68 | 10.3 | 174 | 8.42 | 2.67 | 0.31 | 5.99 | 8.60 |
| 13c2 | 6.59 | 13.3 | 198 | 32.5 | 3.09 | 0.32 | 5.61 | 9.64 |
| 13c3 | <1 | 1.37 | 164 | 23.6 | 2.85 | 0.31 | 5.89 | 9.08 |
| 13c4 | 3.28 | 14.6 | 223 | 8.57 | 3.07 | 0.34 | 5.48 | 8.95 |
| 3 | ≪1 | 0.05 | 190 | 1.24 | 4.46 | 0.31 | 4.39 | 14.2 |
| ETV | <1 | <1 | 127 | 13.2 | 4.19 | 0.40 | 4.10 | 10.4 |

^aMeasured by HPLC. ^bFasted state simulated intestinal fluid. ^cPredicted by the software of ACS/Lab 6.0. ^dCalculated by the formula $-\Delta G/\text{HA}$ (non-hydrogen atom), in which normalizing binding energy $\Delta G = -RT \ln K_d$, presuming $K_d \approx \text{EC}_{50(\text{III})}$. ^eCalculated by the formula $\text{pEC}_{50} - \log P$. ^fCalculated by the formula $\log P/\text{LE}$.

Molecular Modeling Studies. Classical molecular dynamics (MD) simulations were performed to examine the binding mode of 13c2, chosen on the basis of the potent inhibition against NNRTI-resistant strains (Table 4), bound to the NNRTIs binding site in WT HIV-RT. The ligand–protein complex was built up using the X-ray crystallographic structure of the HIV-1 WT RT/K-5a2 complex (PDB code 6C0J) as template.¹³ In the setup of the simulated system, attention was paid to preserve the hydrogen bond between the pyrimidine-bound NH group of 13c2 and the carbonyl oxygen of K101, and the network of hydrogen bonds between the protonated piperidine nitrogen, the backbone carbonyl oxygen of P236 and K103, and a water molecule (W936 in the crystallographic structure).

Three independent MD simulations were run, and the analysis consistently supported the stability of the ligand in the complex (see Figure S1 in Supporting Information), as noted in the resemblance of representative structures of the initial and final binding modes for 13c2 (Figure 3) and the low root-mean square deviation between the energy-minimized average structures sampled along the last 5 ns of the three trajectories (RMSD < 1.4 Å). The benzonitrile moiety is stably accommodated in a hydrophobic pocket formed by Y181, Y188, and W229. The pyrimidine-bound NH of 13c2 is hydrogen-bonded to the carbonyl oxygen of K101 (C=O–HN distance of 2.0 ± 0.2 Å; Supporting Information Figure S2). A network of water-mediated protein–ligand and protein–protein interactions can be observed around the protonated piperidine nitrogen of 13c2. Whereas in the initial structure (Figure 3A) the nitrogen atom is hydrogen-bonded to a water molecule (1.8 Å; see Table S1), which forms additional interactions with the backbone oxygen of K103 (2.4 Å; Table S1) and the NH amide group of P236 (1.9 Å; in Table S1), such a water molecule is displaced along the trajectory, allowing the protonated nitrogen to form a direct hydrogen bond with the backbone oxygen of K103 (1.8 ± 0.2 Å; Figure 3B and Supporting Information Figure S2) while preserving its interactions of the water molecule with K103 and P236 (see Table S1).

The presence of an ordered water molecule around the protonated piperidine nitrogen of 13c2 was confirmed by water density analysis (Figure S2). In this regard, a density isocontour corresponding to the water oxygen atom was visible near the piperidine nitrogen (Figure S2A). The water molecule is slightly shifted relative to the position of the crystallographic water (Figure S2) due to the gradual approach of residues K102–S105 to the ligand.

No stable direct interactions were formed between residues in the “tolerance region I” and the terminal benzamide group of

13c2. This is in contrast with the X-ray structure of the complex with K-5a2, where the sulfonamide group forms hydrogen bonds with the carbonyl oxygen of K104 and the amide NH group of V106. The lack of direct interactions may be ascribed to the lower flexibility of the benzamide moiety in 13c2 upon bioisosteric replacement of the benzosulfonamide group in K-5a2 and to the intrinsic flexibility of residues that shape the pocket filled by the benzamide unit, such as Q222–E224 (Supporting Information Figure S1), in agreement with the high B-factor values observed for these residues in the crystallographic structure.

As noted above, 13c2 can inhibit single (L100I, K103N, Y181C, Y188L, E138K) and double (F227+V106A) mutated HIV-RT variants (see Figure S3 for the location of these mutations). Five mutations (L100I, Y181C, Y188L, F227L, and V106) are located in the hydrophobic pocket that accommodates the benzonitrile and benzamide moieties of the ligand. The inhibitory activity of 13c2 can be justified by the fact that the mutated residues do not reduce the volume filled by these chemical fragments and the preservation of the hydrophobic nature of the pockets. This is supported by the existence of crystallographic complexes of 25a (a ligand similar to K-5a2) with the double mutant F227+V106A (PDB code 6DUF) and with the single mutant Y181I (PDB code 6DUH) of HIV-RT.¹³ Finally, the K103N mutation (Figure S3) is expected to be compatible with binding of 13c2 since local protein–ligand interactions only involve the backbone amide group of residue 103.

Solubility and Lipophilic Efficiency. A potential drug candidate should possess a balance between drug-like properties and potency.¹⁹ Thus, derivatives 13a1 and 13c1–4 were chosen for assessment of certain physicochemical properties. Considering that solubility is important for in vivo dosing formulation and bioavailability, the solubility studies were performed on selected compounds at three different pH values (7.4, 7.0, and 2.0) and fasted state simulated intestinal fluid (FaSSIF). As depicted in Table 7, all the selected compounds displayed excellent solubility at pH 2.0 ($S = 164$ – $223 \mu\text{g/mL}$). Notably, the solubility of 13a1, 13c1, 13c2, and 13c4 ($S = 2.54$ – $14.6 \mu\text{g/mL}$) is much higher than that of 3 and ETV at pH 7.0 and pH 7.4. Furthermore, 13c2 and 13c3 also showed better solubility in FaSSIF ($S = 32.5$ and $23.6 \mu\text{g/mL}$, respectively) compared to that of ETV ($S = 13.2 \mu\text{g/mL}$). These results indicated that the strategy of replacing the aromatic thiophene[3,2-*d*]pyrimidine with nonaromatic fused scaffold has achieved remarkable improvement in compound solubility.

On the other hand, lipophilic efficiency (LE), ligand lipophilic efficiency (LLE), and ligand efficiency dependent lipophilicity

(LELP) are important metrics in medicinal chemistry that have been increasingly applied to guide lead optimization toward drug candidates with critical balance between in vitro efficacy and in vivo drug-like properties.²⁰ Five NNRTI candidates, **13a1**, **13c1**, **13c2**, **13c3**, and **13c4**, were assessed for their lipophilic parameters (Table 7). Inspiringly, **13c1**, **13c2**, **13c3**, and **13c4** with dihydrofuro[3,4-*d*]pyrimidine scaffold satisfy the criteria of all the three ligand lipophilic efficiency indices (LE > 0.3, LLE > 5, LELP < 10).²¹ The results of solubility and lipophilic efficiency demonstrated that the presence of polar dihydrofuran substituents in “tolerant region II” allowed for tuning of lipophilicity to achieve both the desired antiviral activities and optimal physicochemical properties. However, **13a1** with dihydrothieno[3,2-*d*]pyrimidine scaffold showed a lower LLE value of 4.63 and a higher LELP value of 12.4.

CYP Enzymatic Inhibitory Activity. Moreover, the most soluble compound **13c2** was evaluated for its ability to inhibit CYP drug-metabolizing enzymes in vitro. As reported in Table 8,

Table 8. Effects of 13c2 on Inhibition of CYP1A2, CYP2C9, CYP2C19, CYP2D6, and CYP3A4M

| CYP isozyme | standard inhibitor | IC ₅₀ (μM) | compd | IC ₅₀ (μM) |
|-------------|----------------------------------|-----------------------|-------------|-----------------------|
| 1A2 | α-naphthoflavone | 0.194 | 13c2 | >50.0 |
| 2C9 | sulfaphenazole | 0.660 | 13c2 | 46.6 |
| 2C19 | (+)- <i>N</i> -3-benzyl nirvanol | 0.256 | 13c2 | >50.0 |
| 2D6 | quinidine | 0.156 | 13c2 | >50.0 |
| 3A4M | ketoconazole | 0.0366 | 13c2 | >50.0 |

13c2 displayed no significant inhibition of CYP1A2 (IC₅₀ > 50.0 μM), CYP2C9 (IC₅₀ = 46.6 μM), CYP2C19 (IC₅₀ > 50.0 μM), CYP2D6 (IC₅₀ > 50.0 μM), and CYP3A4M (IC₅₀ > 50.0 μM), indicating an unlikely adverse effect on liver.

Determination of Plasma Protein Binding Rate. Furthermore, **13c2** was determined for its binding ability with human and Wistar rat plasma proteins with dialysis equilibrium method, and warfarin was selected as control drug. As shown in Table 9, the plasma protein binding rates of **13c2** were different

Table 9. Plasma Protein Binding Rate of 13c2

| compd | protein-binding rate | | recovery rate | |
|--------------------------|----------------------|--------------------|----------------------|--------------------|
| | human plasma protein | rat plasma protein | human plasma protein | rat plasma protein |
| 13c2 ^a | 93.0% | 91.8% | 86.3% | 77.9% |
| warfarin ^b | 98.5% | 99.1% | 97.5% | 107% |

^aThe concentration of **13c2** is 2 μM. ^bThe concentration of warfarin is 1 μM.

in human and rat and the plasma protein binding rate was about 93.0% and 91.8%, respectively. The result demonstrated that the compound could bind strongly to plasma and there is a low concentration of free drug.

Table 10. Pharmacokinetic Profile of 13c2^a

| subject | T _{1/2} (h) | T _{max} (h) | C _{max} (ng/mL) | AUC _{0-t} (h·ng/mL) | AUC _{0-∞} (h·ng/mL) | CL (L h ⁻¹ kg ⁻¹) | F (%) |
|-------------------------------|----------------------|----------------------|--------------------------|------------------------------|------------------------------|--|-------|
| 13c2 (iv) ^b | 1.09 ± 0.13 | 0.033 | 460 ± 65.9 | 500 ± 17.5 | 543 ± 20.5 | 3.69 | |
| 13c2 (po) ^c | 11.1 ± 0.61 | 1.33 ± 0.22 | 400 ± 76.1 | 1546 ± 114 | 1658 ± 130 | | 30.96 |

^aPK parameters (mean ± SD, n = 5). ^bDosed intravenously at 2 mg/kg. ^cDosed orally at 20 mg/kg.

In Vivo Pharmacokinetics Study. In view of its improved potency against resistance-associated variants and promising physicochemical properties, the pharmacokinetics of compound **13c2** was evaluated after single iv and po administration in Wistar rats. After a single 2 mg/kg iv dose of **13c2**, the mean clearance rate (CL) and half-time (t_{1/2}) was 3.69 L h⁻¹ kg⁻¹ and 1.09 h (Table 10 and Figure 4). Absorption of **13c2** was assessed after being dosed at 20 mg/kg; it reached maximum concentration (T_{max}) at 1.33 h with a maximum concentration (C_{max}) of 400 ng/mL. Notably, the t_{1/2} of **13c2** was up to 11.1 h. The oral bioavailability (F) was 30.96%, which was sufficiently high enough for a drug candidate.

Safety Assessment. Assessment of Acute Toxicity. A single-dose toxicity trial of **13c2** was carried out in Kunming mice. No death occurred after intragastric administration of **13c2** at a dose of 800 mg/kg. Furthermore, there was no significant behavior abnormalities compared to the control group in 2 weeks. All these results support the potential of **13c2** as a novel NNRTI drug candidate with high efficiency, low toxicity, and good oral bioavailability.

Assessment of Subacute Toxicity. The subacute toxicity experiments of **13c2** were carried out to further evaluate their in vivo safety. No behavioral abnormalities were observed during the treatment period of po administered mice treated with 50 mg kg⁻¹ day⁻¹ of **13c2** in 2 weeks. Furthermore, organs toxicity experiments were examined by hematoxylin–eosin (HE) staining. ETV was selected as positive drug. As depicted in Figure 5, there is alveolar interstitial thickening and alveolar hemorrhage (the blue arrow) in the lung and proximal convoluted tubule edema (the red circle) in the kidney after treatment with ETV. After treatment with **13c2**, the results demonstrated that the heart, liver, spleen, lungs, and kidneys of the mice were not damaged.

Assessment of hERG Activity. Compounds with a high affinity for the hERG potassium channel could induce QT interval prolongation, which is frequently related to potentially risk for cardiotoxicity. So we tested the hERG inhibition activity of **13c2** with in vitro manual patch-clamp electrophysiology, and terfenadine was selected as reference drug (Table S2 and Table S3).¹² The result (Figure 6) showed that compound **13c2** (IC₅₀ = 0.83 μM) had much weaker inhibition against the potassium channel, much lower than that of terfenadine (IC₅₀ = 0.086 μM).

CONCLUSION

Starting from our previously described thiophene[3,2-*d*]pyrimidine derivative **3**, a structure-guided scaffold hopping was performed to design structurally diverse derivatives and to explore the chemical space in the “tolerant region I” and “tolerant region II” of the RT NNIBP. SARs of the lead structure were further extended. Encouragingly, the desired antiviral activities and physicochemical properties were achieved with the dihydrofuro[3,4-*d*]pyrimidine scaffold, which was found to lead to a stable binding mode in MD simulations of the ligand-bound complex. Especially, **13c2** and **13c4** proved to be the

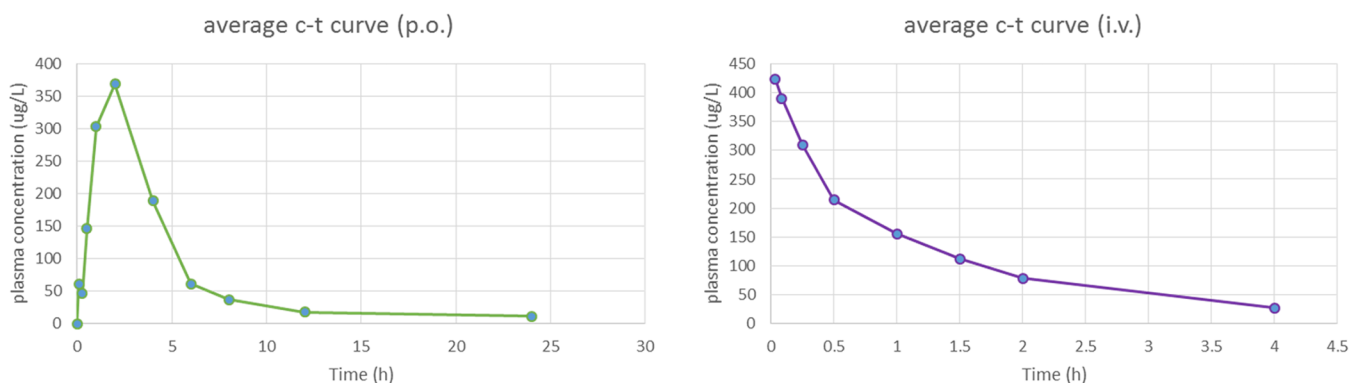


Figure 4. Plasma 13c2 concentration–time profiles in rats following oral administration ($20 \text{ mg}\cdot\text{kg}^{-1}$) and intravenous administration ($2 \text{ mg}\cdot\text{kg}^{-1}$).

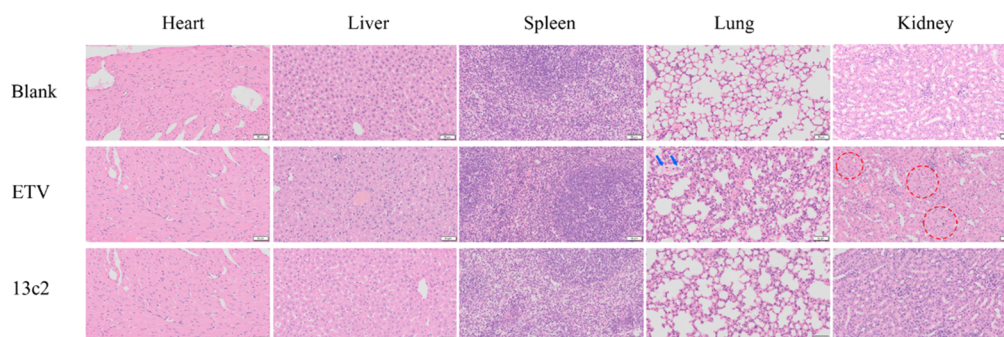


Figure 5. HE of different organs of normal mice with ETV ($50 \text{ mg}/\text{kg}$) and 13c2 ($50 \text{ mg}/\text{kg}$). Scale bars represent $50 \mu\text{m}$.

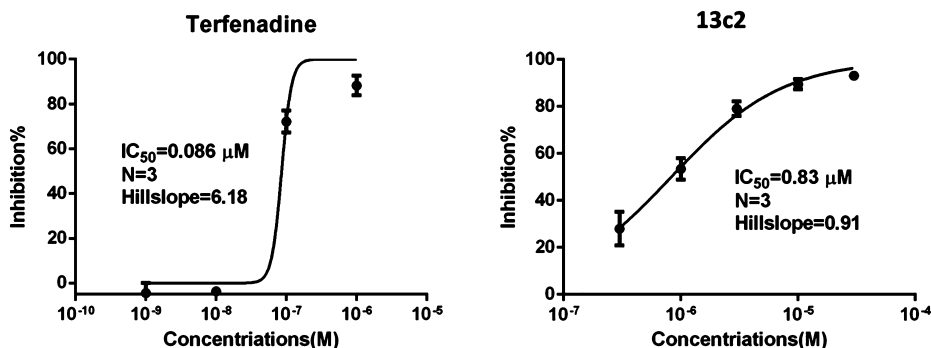


Figure 6. Activity of 13c2 and terfenadine against hERG potassium channel in HEK293 cells.

exceptionally potent inhibitors, exhibiting EC_{50} values of 0.9–7.0 nM against single NNRTI-resistant strains L100I, K103N, Y181C, Y188L, and E138K in MT-4 cells and bringing approximately 1.3- to 3.6 fold improvement in potency compared with ETV ($\text{EC}_{50} = 3.3\text{--}20.4 \text{ nM}$). For double mutant HIV-1 strains F227L+V106A and RES056, both inhibitors displayed comparable activities with those of ETV. Furthermore, 13c2 also had much lower cytotoxicity ($\text{CC}_{50} > 250 \mu\text{M}$), dramatically higher SI values, and low resistance FC values of 0.6–5.3 for single mutant strains. The results of MD simulation studies demonstrated that the bulkier molecular surface contributed to the increased binding affinity and resistance profiles compared with ETV. The CYP enzymatic inhibition test proved that 13c2 has relatively low adverse effect on the liver. The hERG inhibition activity of 13c2 ($\text{IC}_{50} = 0.83 \mu\text{M}$) was a major improvement over terfenadine ($\text{IC}_{50} = 0.086 \mu\text{M}$). Notably, 13c2 exhibited appealing PK profiles, with a low/moderate clearance in rats. The bioavailability of 13c2 is projected to be 30.96%. Taken together, 13c2 is a promising

anti-HIV-1 drug candidate with potent antiviral activities and desirable drug-like properties.

EXPERIMENTAL SECTION

Chemistry. All melting points were determined on a micro melting point apparatus (RY-1G, Tianjin TianGuang Optical Instruments) and are uncorrected. Proton nuclear magnetic resonance (^1H NMR) and carbon nuclear magnetic resonance (^{13}C NMR) spectra were recorded in $\text{DMSO}-d_6$ on a Bruker AV-400 spectrometer with tetramethylsilane (TMS) as the internal standard. Coupling constants are given in hertz, and chemical shifts are reported in δ values (ppm) from TMS; signals are abbreviated as s (singlet), d (doublet), t (triplet), q (quarter), and m (multiplet). A G1313A standard LC autosampler (Agilent) was used to collect samples for measurement of mass spectra. The temperature of the reaction mixture was monitored with a mercury thermometer. All reactions were routinely monitored by thin layer chromatography (TLC) on silica gel GF254 for TLC (Merck), and spots were visualized with iodine vapor or by irradiation with UV light ($\lambda = 254 \text{ nm}$). After completion of each reaction, the mixture was brought to ambient temperature via air-jet cooling. Flash column chromatography was

performed on columns packed with silica gel (200–300 mesh), purchased from Qingdao Haiyang Chemical Company. Solvents were purified and dried by means of standard methods when necessary. Organic solutions were dried over anhydrous sodium sulfate and concentrated with a rotary evaporator under reduced pressure. Other reagents were obtained commercially and were used without further purification. Sample purity was analyzed on a Shimadzu SPD-20A/20AV HPLC system with a Inertsil ODS-SP, 5 μ m C18 column (150 mm \times 4.6 mm). HPLC conditions: methanol/water with 0.1% formic acid 80:20; flow rate 1.0 mL/min; UV detection from 210 to 400 nm; temperature, ambient; injection volume, 20 μ L. 4-((2-Chlorothieno[3,2-*d*]pyrimidin-4-yl)oxy)-3,5-dimethylbenzonitrile (**5**) was prepared as previously reported.¹¹ Purity of all tested compounds was >95%.

4-((2-(Azepan-4-ylamino)thieno[3,2-*d*]pyrimidin-4-yl)oxy)-3,5-dimethylbenzonitrile (7a). A solution of **5** (1.0 g, 3.17 mmol), *tert*-butyl 4-aminoazepane-1-carboxylate (0.81 g, 3.80 mmol), and anhydrous K₂CO₃ (0.87 g, 6.33 mmol) in 15 mL of DMF was heated at 120 °C under magnetic stirring for 8 h. After completion (monitored by TLC), the mixture was cooled to room temperature and 50 mL of ice water was added. The reaction mixture was continuously stirred for another 30 min and the resulting precipitate was collected and dried to give the intermediate **6a**, which was used directly without purification. To a solution of **6a** (0.49 g, 1.0 mmol) in dichloromethane (DCM) (3 mL) was added trifluoroacetic acid (TFA) (1.10 mL, 15 mmol) at room temperature. After the mixture was stirred for 3 h (monitored by TLC), it was alkalinized to pH 9 with saturated sodium bicarbonate solution and washed with saturated salt water (15 mL). The aqueous phase was extracted with DCM (3 \times 5 mL). The combined organic phase was dried over Na₂SO₄. The filtrate was concentrated and purified by column chromatography on silica gel to get **7a** as a white solid with 71% yield. Mp: 86–88 °C. ¹H NMR (400 MHz, DMSO-*d*₆) δ 8.23 (d, *J* = 5.3 Hz, 1H, C₆-thienopyrimidine-H), 7.73 (s, 2H, C₃,C₅-Ph'-H), 7.26 (d, *J* = 5.4 Hz, 1H, C₇-thienopyrimidine-H), 6.81 (s, 1H, NH), 2.96–2.93 (m, 2H), 2.12 (s, 6H), 1.95–1.71 (m, 7H), 1.60–1.52 (m, 2H). ESI-MS: *m/z* 406.4 [M + 1]⁺. C₂₂H₂₃N₅OS (405.16). HPLC purity: 98.26%.

4-((2-((8-Azabicyclo[3.2.1]octan-3-yl)amino)thieno[3,2-*d*]pyrimidin-4-yl)oxy)-3,5-dimethylbenzonitrile (7b). Recrystallized from ethyl acetate (EA)/petroleum ether (PE) as a white solid, 62% yield. Mp: 131–133 °C. ¹H NMR (400 MHz, DMSO-*d*₆) δ 8.22 (d, *J* = 5.4 Hz, 1H, C₆-thienopyrimidine-H), 7.75 (s, 2H, C₃,C₅-Ph-H), 7.25 (d, 1H, C₇-thienopyrimidine-H), 6.89 (s, 1H, NH), 3.96–3.94 (m, 1H), 2.68–2.66 (m, 2H), 2.12 (s, 6H), 1.92–1.14 (m, 8H). ESI-MS: *m/z* 394.5 [M + 1]⁺. C₂₁H₂₃N₅OS (393.16). HPLC purity: 99.28%.

(R)-3,5-Dimethyl-4-((2-(pyrrolidin-3-ylamino)thieno[3,2-*d*]pyrimidin-4-yl)oxy)benzonitrile (7c). Recrystallized from EA/PE as a white solid, 57% yield. Mp: 168–170 °C. ¹H NMR (400 MHz, DMSO-*d*₆) δ 8.21 (d, *J* = 5.4 Hz, 1H, C₆-thienopyrimidine-H), 7.73 (s, 2H, C₃,C₅-Ph-H), 7.25 (d, *J* = 5.4 Hz, 1H, C₇-thienopyrimidine-H), 7.19 (s, 1H, NH), 2.95–2.84 (m, 2H), 2.32–2.28 (m, 2H), 2.08 (s, 6H), 1.65–1.54 (m, 2H). ESI-MS: *m/z* 366.5 [M + 1]⁺. C₁₉H₁₉N₅OS (365.13). HPLC purity: 95.73%.

(S)-3,5-Dimethyl-4-((2-(pyrrolidin-3-ylamino)thieno[3,2-*d*]pyrimidin-4-yl)oxy)benzonitrile (7d). Recrystallized from EA/PE as a white solid, 62% yield. Mp: 151–153 °C. ¹H NMR (400 MHz, DMSO-*d*₆) δ 8.22 (d, *J* = 5.4 Hz, 1H, C₆-thienopyrimidine-H), 7.71 (s, 2H, C₃,C₅-Ph-H), 7.25 (d, *J* = 5.3 Hz, 1H, C₇-thienopyrimidine-H), 7.16 (s, 1H, NH), 4.32 (s, 1H), 2.97–2.91 (m, 2H), 2.38–2.31 (m, 2H), 2.08 (s, 6H), 1.81–1.57 (m, 2H). ESI-MS: *m/z* 366.5 [M + 1]⁺. C₁₉H₁₉N₅OS (365.13). HPLC purity: 99.83%.

4-((2-(Azetidin-3-ylamino)thieno[3,2-*d*]pyrimidin-4-yl)oxy)-3,5-dimethylbenzonitrile (7e). Recrystallized from EA/PE as a white solid, 57% yield. Mp: 132–134 °C. ¹H NMR (400 MHz, DMSO-*d*₆) δ 8.22 (d, *J* = 5.4 Hz, 1H, C₆-thienopyrimidine-H), 7.73 (s, 2H, C₃,C₅-Ph-H), 7.25 (d, *J* = 5.4 Hz, 1H, C₇-thienopyrimidine-H), 7.13 (s, 1H, NH), 4.36 (s, 1H), 3.46–3.43 (m, 2H), 2.98–2.93 (m, 2H), 2.11 (s, 6H). ESI-MS: *m/z* 352.4 [M + 1]⁺. C₁₈H₁₇N₅OS (351.12). HPLC purity: 99.47%.

General Procedure for the Preparation of Final Compounds 8a1–5. To a solution of **7a** (0.5 mmol) in DMF (8 mL) were added

anhydrous K₂CO₃ (0.6 mmol) and substituted benzyl chloride (bromide) (0.55 mmol). After being stirred at ambient temperature for 4–7 h (monitored by TLC), the mixture was poured into water (20 mL) and extracted with ethyl acetate (3 \times 10 mL). The organic phase was washed with saturated sodium chloride (2 \times 10 mL) and then dried over Na₂SO₄. The filtrate was concentrated, purified by column chromatography, and recrystallized from ethyl acetate/petroleum ether to afford the target compounds **8a1–5**.

4-((4-((4-(4-Cyano-2,6-dimethylphenoxy)thieno[3,2-*d*]pyrimidin-2-yl)amino)azepan-1-yl)methyl)benzenesulfonamide (8a1). Recrystallized from EA/PE as a white solid, 59% yield. Mp: 239–241 °C. ¹H NMR (400 MHz, DMSO-*d*₆) δ 8.21 (d, *J* = 5.4 Hz, 1H, C₆-thienopyrimidine-H), 7.87 (d, *J* = 8.0 Hz, 2H, C₃,C₅-Ph'-H), 7.73 (s, 2H, C₃,C₅-Ph''-H), 7.60 (d, *J* = 8.0 Hz, 2H, C₂,C₆-Ph'-H), 7.31 (s, 2H, SO₂NH₂), 7.24 (d, *J* = 5.4 Hz, 1H, C₇-thienopyrimidine-H), 6.80 (s, 1H, NH), 3.56 (s, 2H, N-CH₂), 2.99–2.97 (m, 2H), 2.12 (s, 6H), 1.87–1.75 (m, 7H), 1.60–1.57 (m, 2H). ¹³C NMR (100 MHz, DMSO-*d*₆) δ 161.6, 160.7, 156.4, 150.7, 143.2, 133.2, 132.9, 129.3, 126.1, 123.5, 119.0, 109.0, 58.1, 55.6, 43.3, 35.7, 26.1, 16.2. ESI-MS: *m/z* 575.6 [M + 1]⁺. C₂₉H₃₀N₆O₃S₂ (574.18). HPLC purity: 95.46%.

4-((4-((4-(4-Cyano-2,6-dimethylphenoxy)thieno[3,2-*d*]pyrimidin-2-yl)amino)azepan-1-yl)methyl)benzamide (8a2). Recrystallized from EA/PE as a white solid, 63% yield. Mp: 175–177 °C. ¹H NMR (400 MHz, DMSO-*d*₆) δ 8.20 (d, *J* = 5.4 Hz, 1H, C₆-thienopyrimidine-H), 7.87 (d, *J* = 8.2 Hz, 2H, C₃,C₅-Ph'-H), 7.73 (s, 2H, C₃,C₅-Ph''-H), 7.51 (d, *J* = 8.1 Hz, 2H, C₂,C₆-Ph'-H), 7.40 (s, 2H, CONH₂), 7.25 (d, *J* = 5.4 Hz, 1H, C₇-thienopyrimidine-H), 6.78 (s, 1H, NH), 3.54 (s, 2H, N-CH₂), 3.07–2.88 (m, 2H), 2.11 (s, 6H), 1.99–1.77 (m, 7H), 1.72–1.63 (s, 2H). ¹³C NMR (100 MHz, DMSO-*d*₆) δ 168.4, 161.5, 156.3, 153.7, 150.6, 143.2, 134.7, 133.2, 132.9, 128.4, 126.1, 119.3, 108.6, 62.5, 57.8, 53.4, 36.2, 26.5, 16.2. ESI-MS: *m/z* 539.6 [M + 1]⁺. C₃₀H₃₀N₆O₂S (538.22). HPLC purity: 95.01%.

3-((4-((4-(4-Cyano-2,6-dimethylphenoxy)thieno[3,2-*d*]pyrimidin-2-yl)amino)azepan-1-yl)methyl)benzamide (8a3). Recrystallized from EA/PE as a white solid, 62% yield. Mp: 143–146 °C. ¹H NMR (400 MHz, DMSO-*d*₆) δ 8.20 (d, *J* = 5.4 Hz, 1H, C₆-thienopyrimidine-H), 7.94 (s, 1H, C₂-Ph'-H), 7.75–7.73 (m, 3H), 7.49 (d, *J* = 7.7 Hz, 1H, C₆-Ph'-H), 7.39 (d, *J* = 7.6 Hz, 1H, C₅-Ph'-H), 7.33–7.32 (m, 2H), 7.25 (d, *J* = 5.4 Hz, 1H, C₇-thienopyrimidine-H), 6.78 (s, 1H, NH), 3.55 (s, 2H, N-CH₂), 3.09–2.85 (m, 2H), 2.11 (s, 6H), 1.99–1.78 (m, 7H), 1.64 (s, 2H). ¹³C NMR (100 MHz, DMSO-*d*₆) δ 168.5, 160.7, 156.3, 150.7, 143.2, 134.6, 133.2, 132.9, 128.4, 126.1, 119.2, 108.6, 61.8, 57.8, 53.4, 36.2, 26.5, 16.2. ESI-MS: *m/z* 539.6 [M + 1]⁺. C₃₀H₃₀N₆O₂S (538.22). HPLC purity: 96.12%.

3,5-Dimethyl-4-((2-((1-(4-(methylsulfonyl)benzyl)azepan-4-yl)amino)thieno[3,2-*d*]pyrimidin-4-yl)oxy)benzonitrile (8a4). Recrystallized from EA/PE as a white solid, 67% yield. Mp: 118–120 °C. ¹H NMR (400 MHz, DMSO-*d*₆) δ 8.21 (d, *J* = 5.4 Hz, 1H, C₆-thienopyrimidine-H), 7.87 (d, *J* = 8.0 Hz, 2H, C₃,C₅-Ph'-H), 7.73 (s, 2H, C₃,C₅-Ph''-H), 7.61 (d, *J* = 8.0 Hz, 2H, C₂,C₆-Ph'-H), 7.25 (d, *J* = 5.4 Hz, 1H, C₇-thienopyrimidine-H), 6.80 (s, 1H, NH), 3.55 (s, 2H, N-CH₂), 3.20 (s, 3H, SO₂CH₃), 2.98 (s, 2H), 2.12 (s, 6H), 1.90–1.81 (m, 7H), 1.67–1.63 (m, 2H). ¹³C NMR (100 MHz, DMSO-*d*₆) δ 165.8, 160.7, 153.4, 147.1, 139.5, 133.2, 132.9, 129.3, 127.3, 123.5, 119.0, 109.0, 58.1, 55.6, 44.1, 43.3, 35.7, 26.1, 16.2. ESI-MS: *m/z* 574.5 [M + 1]⁺. C₃₀H₃₁N₅O₃S₂ (573.19). HPLC purity: 95.78%.

3,5-Dimethyl-4-((2-((1-(pyridin-4-ylmethyl)azepan-4-yl)amino)thieno[3,2-*d*]pyrimidin-4-yl)oxy)benzonitrile (8a5). Recrystallized from EA/PE as a white solid, 63% yield. Mp: 246–248 °C. ¹H NMR (400 MHz, DMSO-*d*₆) δ 8.50 (d, *J* = 5.0 Hz, 2H, C₃,C₅-Py-H), 8.21 (d, *J* = 5.4 Hz, 1H, C₆-thienopyrimidine-H), 7.73 (s, 2H, C₃,C₅-Ph'-H), 7.31 (d, *J* = 5.1 Hz, 2H, C₂,C₆-Py-H), 7.25 (d, *J* = 5.4 Hz, 1H, C₇-thienopyrimidine-H), 6.87 (s, 1H, NH), 3.55 (s, 2H, N-CH₂), 2.98–2.96 (s, 2H), 2.12 (s, 6H), 1.90–1.77 (m, 7H), 1.65–1.54 (m, 2H). ¹³C NMR (100 MHz, DMSO-*d*₆) δ 165.8, 160.7, 153.4, 151.6, 149.9, 139.5, 133.2, 132.9, 129.4, 127.3, 123.5, 119.0, 109.0, 58.1, 55.6, 43.4, 35.7, 26.1, 16.2. ESI-MS: *m/z* 497.6 [M + 1]⁺. C₂₈H₂₈N₆OS (496.20). HPLC purity: 98.69%.

4-((3-((4-(4-Cyano-2,6-dimethylphenoxy)thieno[3,2-d]pyrimidin-2-yl)amino)-8-azabicyclo[3.2.1]octan-8-yl)methyl)benzenesulfonamide (8b1). Recrystallized from EA/PE as a white solid, 76% yield. Mp: 115–117 °C. ¹H NMR (400 MHz, DMSO-*d*₆) δ 8.20 (d, *J* = 5.4 Hz, 1H, C₆-thienopyrimidine-H), 7.78 (d, *J* = 7.9 Hz, 2H, C₃,C₅-Ph'-H), 7.73 (s, 2H, C₃,C₅-Ph''-H), 7.48 (d, *J* = 8.0 Hz, 2H, C₂,C₆-Ph'-H), 7.31 (s, 2H, SO₂NH₂), 7.24–7.23 (m, 1H, C₇-thienopyrimidine-H), 6.89 (s, 1H, NH), 4.09–3.93 (m, 1H), 3.61 (s, 2H, N-CH₂), 2.72–2.65 (m, 2H), 2.12 (s, 6H), 1.92–1.14 (m, 8H). ¹³C NMR (100 MHz, DMSO-*d*₆) δ 161.7, 160.2, 156.4, 154.7, 150.8, 143.0, 133.2, 132.9, 129.1, 126.0, 119.0, 109.0, 61.9, 53.8, 34.3, 32.9, 25.0, 16.2. ESI-MS: *m/z* 563.5 [M + 1]⁺. C₂₈H₃₀N₆O₃S₂ (562.18). HPLC purity: 98.43%.

4-((3-((4-(4-Cyano-2,6-dimethylphenoxy)thieno[3,2-d]pyrimidin-2-yl)amino)-8-azabicyclo[3.2.1]octan-8-yl)methyl)benzamide (8b2). Recrystallized from EA/PE as a white solid, 65% yield. Mp: 103–105 °C. ¹H NMR (400 MHz, DMSO-*d*₆) δ 8.20 (d, *J* = 5.3 Hz, 1H, C₆-thienopyrimidine-H), 7.79 (d, *J* = 8.1 Hz, 2H, C₃,C₅-Ph'-H), 7.73 (s, 2H, C₃,C₅-Ph''-H), 7.49 (d, *J* = 8.0 Hz, 2H, C₂,C₆-Ph'-H), 7.30 (s, 2H, CONH₂), 7.24–7.23 (m, 1H, C₇-thienopyrimidine-H), 6.89 (s, 1H, NH), 4.01–3.93 (m, 1H), 3.62 (s, 2H, N-CH₂), 2.72–2.70 (m, 2H), 2.12 (s, 6H), 1.89–1.21 (m, 8H). ¹³C NMR (100 MHz, DMSO-*d*₆) δ 168.5, 161.7, 156.4, 154.7, 150.8, 143.0, 133.2, 132.9, 129.7, 126.2, 119.0, 109.0, 61.9, 53.8, 32.9, 25.0, 16.2. ESI-MS: *m/z* 527.6 [M + 1]⁺. C₂₉H₃₀N₆O₂S (526.22). HPLC purity: 97.15%.

3-((3-((4-(4-Cyano-2,6-dimethylphenoxy)thieno[3,2-d]pyrimidin-2-yl)amino)-8-azabicyclo[3.2.1]octan-8-yl)methyl)benzamide (8b3). Recrystallized from EA/PE as a white solid, 61% yield. Mp: 162–164 °C. ¹H NMR (400 MHz, DMSO-*d*₆) δ 8.20 (d, *J* = 5.4 Hz, 1H, C₆-thienopyrimidine-H), 7.79 (s, 1H, C₂-Ph'-H), 7.74–7.73 (m, 3H), 7.44 (d, *J* = 7.4 Hz, 1H, C₆-Ph'-H), 7.39 (d, *J* = 7.5 Hz, 1H, C₅-Ph'-H), 7.34 (s, 2H, CONH₂), 7.24–7.23 (m, 1H, C₇-thienopyrimidine-H), 6.88 (s, 1H, NH), 4.06–4.04 (m, 1H), 3.57 (s, 2H, N-CH₂), 2.75–2.68 (m, 2H), 2.12 (s, 6H), 1.90–1.58 (s, 8H). ¹³C NMR (100 MHz, DMSO-*d*₆) δ 168.4, 156.8, 153.4, 150.2, 143.1, 140.2, 134.6, 133.2, 132.9, 131.7, 128.4, 128.2, 126.3, 119.0, 62.3, 40.5, 33.0, 25.0, 16.2. ESI-MS: *m/z* 527.6 [M + 1]⁺. C₂₉H₃₀N₆O₂S (526.22). HPLC purity: 98.98%.

3,5-Dimethyl-4-((2-((8-(4-(methylsulfonyl)benzyl)-8-azabicyclo[3.2.1]octan-3-yl)amino)thieno[3,2-d]pyrimidin-4-yl)oxy)benzoxazole (8b4). Recrystallized from EA/PE as a white solid, 72% yield. Mp: 114–116 °C. ¹H NMR (400 MHz, DMSO-*d*₆) δ 8.21 (d, *J* = 5.4 Hz, 1H, C₆-thienopyrimidine-H), 7.90 (d, *J* = 8.0 Hz, 2H, C₃,C₅-Ph'-H), 7.73 (s, 2H, C₃,C₅-Ph''-H), 7.58 (d, *J* = 8.0 Hz, 2H, C₂,C₆-Ph'-H), 7.24–7.23 (m, 1H, C₇-thienopyrimidine-H), 6.90 (s, 1H, NH), 4.20–3.95 (m, 1H), 3.62 (s, 2H, N-CH₂), 3.22 (s, 3H, SO₂CH₃), 2.72–2.67 (m, 2H), 2.12 (s, 6H), 1.92–1.35 (m, 8H). ¹³C NMR (100 MHz, DMSO-*d*₆) δ 163.2, 156.8, 153.4, 149.2, 145.0, 139.4, 138.0, 137.3, 136.4, 133.8, 133.2, 132.9, 131.0, 123.7, 113.8, 67.0, 40.5, 37.8, 33.0, 25.0, 16.2. ESI-MS: *m/z* 562.6 [M + 1]⁺. C₂₉H₃₁N₅O₃S₂ (561.19). HPLC purity: 98.26%.

3,5-Dimethyl-4-((2-((8-(pyridin-4-ylmethyl)-8-azabicyclo[3.2.1]octan-3-yl)amino)thieno[3,2-d]pyrimidin-4-yl)oxy)benzoxazole (8b5). Recrystallized from EA/PE as a white solid, 70% yield. Mp: 96–98 °C. ¹H NMR (400 MHz, DMSO-*d*₆) δ 8.50 (d, *J* = 5.1 Hz, 2H, C₃,C₅-Py-H), 8.21 (d, *J* = 5.3 Hz, 1H, C₆-thienopyrimidine-H), 7.73 (s, 2H, C₃,C₅-Ph'-H), 7.30 (d, *J* = 4.9 Hz, 2H, C₂,C₆-Py-H), 7.24–7.23 (s, 1H, C₇-thienopyrimidine-H), 6.89 (s, 1H, NH), 4.07–4.04 (m, 1H), 3.58 (s, 2H, N-CH₂), 2.72–2.67 (m, 2H), 2.12 (s, 6H), 1.95–1.08 (m, 8H). ¹³C NMR (100 MHz, DMSO-*d*₆) δ 160.8, 156.7, 154.0, 151.2, 149.9, 133.2, 132.9, 126.5, 123.8, 119.0, 109.0, 61.3, 39.6, 34.2, 33.0, 25.0, 16.2. ESI-MS: *m/z* 485.7 [M + 1]⁺. C₂₇H₂₈N₆O₃S (484.20). HPLC purity: 98.44%.

(R)-4-((3-((4-(4-Cyano-2,6-dimethylphenoxy)thieno[3,2-d]pyrimidin-2-yl)amino)pyrrolidin-1-yl)methyl)benzenesulfonamide (8c1). Recrystallized from EA/PE as a white solid, 54% yield. Mp: 138–140 °C. ¹H NMR (400 MHz, DMSO-*d*₆) δ 8.21 (d, *J* = 5.4 Hz, 1H, C₆-thienopyrimidine-H), 7.77 (d, *J* = 8.0 Hz, 2H, C₃,C₅-Ph'-H), 7.73 (s, 2H, C₃,C₅-Ph''-H), 7.46 (d, *J* = 7.9 Hz, 2H, C₂,C₆-Ph'-H), 7.31 (s, 2H, SO₂NH₂), 7.25 (d, *J* = 5.4 Hz, 1H, C₇-thienopyrimidine-H), 7.19 (s, 1H, NH), 3.60 (s, 2H, N-CH₂), 3.02–

2.80 (m, 2H), 2.30–2.29 (m, 2H), 2.08 (s, 6H), 1.79–1.19 (m, 2H). ¹³C NMR (100 MHz, DMSO-*d*₆) δ 153.4, 143.7, 143.1, 133.2, 133.0, 132.9, 129.2, 126.0, 119.0, 109.0, 60.4, 59.3, 52.9, 30.9, 16.2. ESI-MS: *m/z* 535.6 [M + 1]⁺. C₂₆H₂₆N₆O₃S₂ (534.15). HPLC purity: 98.49%.

(R)-4-((3-((4-(4-Cyano-2,6-dimethylphenoxy)thieno[3,2-d]pyrimidin-2-yl)amino)pyrrolidin-1-yl)methyl)benzamide (8c2). Recrystallized from EA/PE as a white solid, 50% yield. Mp: 119–121 °C. ¹H NMR (400 MHz, DMSO-*d*₆) δ 8.21 (d, *J* = 5.4 Hz, 1H, C₆-thienopyrimidine-H), 7.82 (d, *J* = 7.8 Hz, 2H, C₃,C₅-Ph'-H), 7.69 (s, 2H, C₃,C₅-Ph''-H), 7.34 (d, *J* = 8.0 Hz, 2H, C₂,C₆-Ph'-H), 7.25 (s, 2H, CONH₂), 7.24 (d, *J* = 5.4 Hz, 1H, C₇-thienopyrimidine-H), 7.16 (s, 1H, NH), 4.30 (s, 1H), 3.56 (s, 2H, N-CH₂), 2.89–2.80 (m, 2H), 2.32–2.25 (m, 2H), 2.08 (s, 6H), 1.92–1.19 (m, 2H). ¹³C NMR (101 MHz, DMSO-*d*₆) δ 168.2, 153.4, 133.2, 132.9, 128.7, 127.8, 119.0, 109.0, 60.4, 52.9, 39.6, 39.4, 30.9, 16.2. ESI-MS: *m/z* 499.3 [M + 1]⁺. C₂₆H₂₆N₆O₃S₂ (498.18). HPLC purity: 97.20%.

(R)-3-((3-((4-(4-Cyano-2,6-dimethylphenoxy)thieno[3,2-d]pyrimidin-2-yl)amino)pyrrolidin-1-yl)methyl)benzamide (8c3). Recrystallized from EA/PE as a white solid, 53% yield. Mp: 125–126 °C. ¹H NMR (400 MHz, DMSO-*d*₆) δ 8.20 (d, *J* = 5.4 Hz, 1H, C₆-thienopyrimidine-H), 7.78–7.76 (m, 2H), 7.69 (s, 2H, C₃,C₅-Ph'-H), 7.43–7.38 (m, 2H), 7.34 (s, 2H, CONH₂), 7.25 (d, *J* = 5.4 Hz, 1H, C₇-thienopyrimidine-H), 7.14 (s, 1H, NH), 4.31 (s, 1H), 3.56 (s, 2H, N-CH₂), 2.84–2.80 (m, 2H), 2.32–2.27 (m, 2H), 2.08 (s, 6H), 1.86–1.52 (m, 2H). ¹³C NMR (100 MHz, DMSO-*d*₆) δ 168.3, 162.4, 153.4, 134.6, 133.2, 132.9, 131.9, 128.5, 128.2, 126.4, 109.0, 60.4, 59.8, 52.9, 39.6, 39.4, 30.9, 16.1. ESI-MS: *m/z* 499.3 [M + 1]⁺. C₂₆H₂₆N₆O₃S₂ (498.18). HPLC purity: 96.75%.

(R)-3,5-Dimethyl-4-((2-((1-(4-(methylsulfonyl)benzyl)pyrrolidin-3-yl)amino)thieno[3,2-d]pyrimidin-4-yl)oxy)benzoxazole (8c4). Recrystallized from EA/PE as a white solid, 59% yield. Mp: 125–127 °C. ¹H NMR (400 MHz, DMSO-*d*₆) δ 8.21 (d, *J* = 5.4 Hz, 1H, C₆-thienopyrimidine-H), 7.88 (d, *J* = 8.0 Hz, 2H, C₃,C₅-Ph'-H), 7.69 (s, 2H, C₃,C₅-Ph''-H), 7.55 (d, *J* = 8.0 Hz, 2H, C₂,C₆-Ph'-H), 7.25 (d, *J* = 5.6 Hz, 1H, C₇-thienopyrimidine-H), 7.14 (s, 1H, NH), 4.32 (s, 1H), 3.65 (s, 2H, N-CH₂), 3.21 (s, 3H, SO₂CH₃), 2.88–2.85 (m, 2H), 2.31–2.27 (m, 2H), 2.08 (s, 6H), 1.87–1.51 (m, 2H). ¹³C NMR (100 MHz, DMSO-*d*₆) δ 162.4, 160.7, 153.4, 139.8, 133.2, 132.9, 129.6, 127.3, 127.0, 119.0, 109.0, 60.4, 59.2, 52.9, 44.0, 39.6, 39.4, 31.0, 16.1. ESI-MS: *m/z* 534.6 [M + 1]⁺. C₂₇H₂₇N₅O₃S₂ (533.16). HPLC purity: 96.16%.

(R)-3,5-Dimethyl-4-((2-((1-(pyridin-4-ylmethyl)pyrrolidin-3-yl)amino)thieno[3,2-d]pyrimidin-4-yl)oxy)benzoxazole (8c5). Recrystallized from EA/PE as a white solid, 55% yield. Mp: 174–176 °C. ¹H NMR (400 MHz, DMSO-*d*₆) δ 8.50 (d, *J* = 4.9 Hz, 2H, C₃,C₅-Py-H), 8.21 (d, *J* = 5.4 Hz, 1H, C₆-thienopyrimidine-H), 7.69 (s, 2H, C₃,C₅-Ph'-H), 7.29 (d, *J* = 5.1 Hz, 2H, C₂,C₆-Py-H), 7.25 (d, *J* = 5.5 Hz, 1H, C₇-thienopyrimidine-H), 7.14 (s, 1H, NH), 4.32 (s, 1H), 3.54 (s, 2H, N-CH₂), 2.87–2.86 (m, 2H), 2.30–2.29 (m, 2H), 2.08 (s, 6H), 1.72–1.65 (m, 2H). ¹³C NMR (100 MHz, DMSO-*d*₆) δ 162.4, 153.4, 149.9, 148.5, 133.2, 132.9, 123.9, 119.0, 109.0, 60.4, 58.7, 53.0, 31.0, 16.2. ESI-MS: *m/z* 457.4 [M + 1]⁺. C₂₅H₂₄N₆O₃S (456.17). HPLC purity: 97.20%.

(S)-4-((3-((4-(4-Cyano-2,6-dimethylphenoxy)thieno[3,2-d]pyrimidin-2-yl)amino)pyrrolidin-1-yl)methyl)benzenesulfonamide (8d1). Recrystallized from EA/PE as a white solid, 53% yield. Mp: 129–131 °C. ¹H NMR (400 MHz, DMSO-*d*₆) δ 8.21 (d, *J* = 5.4 Hz, 1H, C₆-thienopyrimidine-H), 7.78 (d, *J* = 8.2 Hz, 2H, C₃,C₅-Ph'-H), 7.70 (s, 2H, C₃,C₅-Ph''-H), 7.46 (d, *J* = 7.6 Hz, 2H, C₂,C₆-Ph'-H), 7.31 (s, 2H, SO₂NH₂), 7.25 (d, *J* = 5.3 Hz, 1H, C₇-thienopyrimidine-H), 7.17 (s, 1H, NH), 4.32 (s, 1H), 3.60 (s, 2H, N-CH₂), 3.10–2.89 (m, 2H), 2.41–2.23 (m, 2H), 2.08 (s, 6H), 1.89–1.54 (m, 2H). ¹³C NMR (100 MHz, DMSO-*d*₆) δ 153.4, 143.1, 133.2, 132.9, 132.7, 129.3, 129.2, 126.1, 126.0, 123.9, 119.0, 109.0, 60.3, 59.3, 52.9, 30.9, 16.2. ESI-MS: *m/z* 535.5 [M + 1]⁺. C₂₆H₂₆N₆O₃S₂ (534.15). HPLC purity: 97.93%.

(S)-4-((3-((4-(4-Cyano-2,6-dimethylphenoxy)thieno[3,2-d]pyrimidin-2-yl)amino)pyrrolidin-1-yl)methyl)benzamide (8d2). Recrystallized from EA/PE as a white solid, 49% yield. Mp: 130–132 °C. ¹H NMR (400 MHz, DMSO-*d*₆) δ 8.20 (d, *J* = 5.4 Hz, 1H, C₆-thienopyrimidine-H), 7.83 (d, *J* = 8.1 Hz, 2H, C₃,C₅-Ph'-H),

7.72–7.65 (m, 2H, C₃C₅-Ph''-H), 7.36–7.29 (m, 2H), 7.25 (d, *J* = 5.4 Hz, 1H, C₇-thienopyrimidine-H), 7.19 (s, 1H, NH), 4.29 (s, 1H), 3.57 (s, 2H, N-CH₂), 2.85–2.67 (m, 2H), 2.32–2.25 (m, 2H), 2.08 (s, 6H), 1.72–1.52 (s, 2H). ¹³C NMR (100 MHz, DMSO-*d*₆) δ 168.2, 153.4, 133.3, 133.2, 132.9, 128.7, 128.6, 127.9, 127.8, 119.0, 109.0, 60.4, 59.5, 52.9, 39.6, 30.9, 16.2. ESI-MS: *m/z* 499.4 [M + 1]⁺. C₂₆H₂₆N₆O₃S₂ (498.18). HPLC purity: 98.11%.

(S)-3-((3-((4-(4-Cyano-2,6-dimethylphenoxy)thieno[3,2-*d*]pyrimidin-2-yl)amino)pyrrolidin-1-yl)methyl)benzamide (8d3). Recrystallized from EA/PE as a white solid, 53% yield. Mp: 109–111 °C. ¹H NMR (400 MHz, DMSO-*d*₆) δ 8.20 (d, *J* = 5.4 Hz, 1H, C₆-thienopyrimidine-H), 7.81–7.74 (m, 2H), 7.69 (s, 2H, C₃C₅-Ph''-H), 7.42–7.41 (m, 2H), 7.34 (s, 2H, CONH₂), 7.25 (d, *J* = 5.4 Hz, 1H, C₇-thienopyrimidine-H), 7.16 (s, 1H, NH), 4.30 (s, 1H), 3.56 (s, 2H, N-CH₂), 2.85–2.81 (m, 2H), 2.30–2.26 (m, 2H), 2.08 (s, 6H), 1.72–1.68 (m, 2H). ¹³C NMR (100 MHz, DMSO-*d*₆) δ 168.3, 160.8, 134.6, 133.2, 132.9, 131.9, 128.5, 128.2, 126.4, 119.0, 109.0, 60.4, 59.8, 52.9, 39.4, 30.9, 16.1. ESI-MS: *m/z* 499.5 [M + 1]⁺. C₂₆H₂₆N₆O₃S₂ (498.18). HPLC purity: 95.73%.

(S)-3,5-Dimethyl-4-((2-((1-(4-(methylsulfonyl)benzyl)pyrrolidin-3-yl)amino)thieno[3,2-*d*]pyrimidin-4-yl)oxy)benzonitrile (8d4). Recrystallized from EA/PE as a white solid, 61% yield. Mp: 95–98 °C. ¹H NMR (400 MHz, DMSO-*d*₆) δ 8.20 (d, *J* = 5.3 Hz, 1H, C₆-thienopyrimidine-H), 7.87 (d, *J* = 8.0 Hz, 2H, C₃C₅-Ph''-H), 7.69 (s, 2H, C₃C₅-Ph''-H), 7.55 (d, *J* = 7.9 Hz, 2H, C₂C₆-Ph''-H), 7.25 (d, *J* = 5.5 Hz, 1H, C₇-thienopyrimidine-H), 7.14 (s, 1H, NH), 4.32 (s, 1H), 3.65 (s, 2H, N-CH₂), 3.22 (s, 3H, SO₂CH₃), 2.87–2.79 (m, 2H), 2.30–2.28 (m, 2H), 2.08 (s, 6H), 1.79–1.48 (m, 2H). ¹³C NMR (100 MHz, DMSO-*d*₆) δ 162.7, 160.7, 153.4, 139.8, 133.2, 132.9, 129.6, 127.4, 127.0, 119.0, 109.1, 60.4, 59.2, 53.0, 44.0, 39.4, 30.8, 16.1. ESI-MS: *m/z* 534.0 [M + 1]⁺. C₂₇H₂₇N₅O₃S₂ (533.16). HPLC purity: 95.81%.

(S)-3,5-Dimethyl-4-((2-((1-(pyridin-4-ylmethyl)pyrrolidin-3-yl)amino)thieno[3,2-*d*]pyrimidin-4-yl)oxy)benzonitrile (8d5). Recrystallized from EA/PE as a white solid, 54% yield. Mp: 184–486 °C. ¹H NMR (400 MHz, DMSO-*d*₆) δ 8.51 (d, *J* = 4.9 Hz, 2H, C₃C₅-Py-H), 8.21 (d, *J* = 5.4 Hz, 1H, C₆-thienopyrimidine-H), 7.69 (s, 2H, C₃C₅-Ph''-H), 7.29 (d, *J* = 4.9 Hz, 2H, C₂C₆-Py-H), 7.25 (d, *J* = 5.5 Hz, 1H, C₇-thienopyrimidine-H), 7.14 (s, 1H, NH), 4.32 (s, 1H), 3.54 (s, 2H, N-CH₂), 2.86–2.84 (m, 2H), 2.30–2.28 (m, 2H), 2.08 (s, 6H), 1.82–1.63 (m, 2H). ¹³C NMR (100 MHz, DMSO-*d*₆) δ 162.4, 153.5, 149.9, 148.5, 133.1, 132.9, 124.0, 119.1, 109.0, 60.3, 58.7, 53.1, 31.2, 16.2. ESI-MS: *m/z* 457.4 [M + 1]⁺. C₂₅H₂₄N₆O₃S (456.17). HPLC purity: 99.42%.

4-((3-((4-(4-Cyano-2,6-dimethylphenoxy)thieno[3,2-*d*]pyrimidin-2-yl)amino)azetid-1-yl)methyl)benzenesulfonamide (8e1). Recrystallized from EA/PE as a white solid, 63% yield. Mp: 130–1321 °C. ¹H NMR (400 MHz, DMSO-*d*₆) δ 8.22 (d, *J* = 5.4 Hz, 1H, C₆-thienopyrimidine-H), 7.76 (d, *J* = 8.2 Hz, 2H, C₃C₅-Ph''-H), 7.73 (s, 2H, C₃C₅-Ph''-H), 7.42 (d, *J* = 8.0 Hz, 2H, C₂C₆-Ph''-H), 7.30 (s, 2H, SO₂NH₂), 7.26 (d, *J* = 5.4 Hz, 1H, C₇-thienopyrimidine-H), 7.13 (s, 1H, NH), 4.37 (s, 1H), 3.60 (s, 2H, N-CH₂), 3.46–3.43 (m, 2H), 2.98–2.96 (m, 2H), 2.11 (s, 6H). ¹³C NMR (100 MHz, DMSO-*d*₆) δ 153.3, 143.2, 143.0, 133.2, 133.0, 128.7, 126.0, 125.9, 119.0, 109.1, 62.5, 61.2, 40.4, 16.2. ESI-MS: *m/z* 521.3 [M + 1]⁺. C₂₃H₂₄N₆O₃S₂ (520.14). HPLC purity: 96.26%.

4-((3-((4-(4-Cyano-2,6-dimethylphenoxy)thieno[3,2-*d*]pyrimidin-2-yl)amino)azetid-1-yl)methyl)benzamide (8e2). Recrystallized from EA/PE as a white solid, 66% yield. Mp: 143–145 °C. ¹H NMR (400 MHz, DMSO-*d*₆) δ 8.22 (d, *J* = 5.4 Hz, 1H, C₆-thienopyrimidine-H), 7.81 (d, *J* = 8.0 Hz, 2H, C₃C₅-Ph''-H), 7.72 (s, 2H, C₃C₅-Ph''-H), 7.48 (s, 2H, CONH₂), 7.30 (d, *J* = 7.0 Hz, 2H, C₂C₆-Ph''-H), 7.26 (d, *J* = 5.4 Hz, 1H, C₇-thienopyrimidine-H), 7.12 (s, 1H, NH), 4.39 (s, 1H), 3.58 (s, 2H, N-CH₂), 3.47–2.46 (m, 2H), 2.93–2.91 (m, 2H), 2.11 (s, 6H). ¹³C NMR (101 MHz, DMSO-*d*₆) δ 168.2, 162.5, 153.3, 143.2, 133.2, 133.0, 128.2, 127.9, 125.9, 119.0, 109.1, 62.5, 61.2, 40.4, 16.2. ESI-MS: *m/z* 485.5 [M + 1]⁺. C₂₆H₂₄N₆O₂S (484.17). HPLC purity: 95.66%.

3-((3-((4-(4-Cyano-2,6-dimethylphenoxy)thieno[3,2-*d*]pyrimidin-2-yl)amino)azetid-1-yl)methyl)benzamide (8e3). Recrystallized from EA/PE as a white solid, 62% yield. Mp: 210–212

°C. ¹H NMR (400 MHz, DMSO-*d*₆) δ 8.21 (d, *J* = 5.3 Hz, 1H, C₆-thienopyrimidine-H), 7.82–7.76 (m, 2H), 7.68 (s, 2H, C₃C₅-Ph''-H), 7.43–7.42 (m, 2H), 7.37 (s, 2H, CONH₂), 7.26 (d, *J* = 5.4 Hz, 1H, C₇-thienopyrimidine-H), 7.13 (s, 1H, NH), 4.38 (s, 1H), 3.57 (s, 2H, N-CH₂), 3.46–3.43 (m, 2H), 2.96–2.94 (m, 2H), 2.08 (s, 6H). ¹³C NMR (100 MHz, DMSO-*d*₆) δ 168.2, 162.5, 153.3, 143.2, 133.1, 132.8, 128.2, 128.0, 125.9, 119.0, 109.1, 62.5, 61.2, 40.4, 16.2. ESI-MS: *m/z* 485.4 [M + 1]⁺. C₂₆H₂₄N₆O₂S (484.17). HPLC purity: 98.24%.

3,5-Dimethyl-4-((2-((1-(4-(methylsulfonyl)benzyl)azetid-3-yl)amino)thieno[3,2-*d*]pyrimidin-4-yl)oxy)benzonitrile (8e4). Recrystallized from EA/PE as a white solid, 55% yield. Mp: 175–177 °C. ¹H NMR (400 MHz, DMSO-*d*₆) δ 8.21 (d, *J* = 5.3 Hz, 1H, C₆-thienopyrimidine-H), 7.77 (d, *J* = 8.0 Hz, 2H, C₃C₅-Ph''-H), 7.73 (s, 2H, C₃C₅-Ph''-H), 7.43 (d, *J* = 7.9 Hz, 2H, C₂C₆-Ph''-H), 7.25 (d, *J* = 5.5 Hz, 1H, C₇-thienopyrimidine-H), 7.14 (s, 1H, NH), 4.36 (s, 1H), 3.61 (s, 2H, N-CH₂), 3.46–3.43 (m, 2H), 3.22 (s, 3H, SO₂CH₃), 2.98–2.95 (m, 2H), 2.08 (s, 6H). ¹³C NMR (100 MHz, DMSO-*d*₆) δ 153.2, 143.3, 143.1, 133.2, 133.0, 128.7, 126.0, 125.7, 119.0, 109.1, 62.7, 61.3, 40.5, 16.2. ESI-MS: *m/z* 520.4 [M + 1]⁺. C₂₆H₂₅N₅O₃S₂ (519.14). HPLC purity: 95.01%.

3,5-Dimethyl-4-((2-((1-(pyridin-4-ylmethyl)azetid-3-yl)amino)thieno[3,2-*d*]pyrimidin-4-yl)oxy)benzonitrile (8e5). Recrystallized from EA/PE as a white solid, 61% yield. Mp: 199–201 °C. ¹H NMR (400 MHz, DMSO-*d*₆) δ 8.52 (d, *J* = 4.9 Hz, 2H, C₃C₅-Py-H), 8.21 (d, *J* = 5.3 Hz, 1H, C₆-thienopyrimidine-H), 7.71 (s, 2H, C₃C₅-Ph''-H), 7.29 (d, *J* = 4.9 Hz, 2H, C₂C₆-Py-H), 7.25 (d, *J* = 5.5 Hz, 1H, C₇-thienopyrimidine-H), 7.15 (s, 1H, NH), 4.32 (s, 1H), 3.54 (s, 2H, N-CH₂), 3.45–3.43 (m, 2H), 2.97–2.96 (m, 2H), 2.08 (s, 6H). ¹³C NMR (100 MHz, DMSO-*d*₆) δ 162.4, 153.5, 149.9, 148.5, 133.1, 132.9, 124.0, 119.1, 109.0, 62.7, 61.2, 40.4, 16.2. ESI-MS: *m/z* 443.5 [M + 1]⁺. C₂₄H₂₂N₆O₃S (442.16). HPLC purity: 95.78%.

General Procedure for the Preparation of Compounds 10a–f. 4-((2-Chloro-6,7-dihydrothieno[3,2-*d*]pyrimidin-4-yl)oxy)-3,5-dimethylbenzonitrile (10a). The synthetic method was similar to that described for IIIA-2 except that the starting material was 2,4-dichloro-6,7-dihydrothieno[3,2-*d*]pyrimidine (9a). Recrystallized from EA/PE as a white solid, 86% yield. Mp: 272–274 °C. ¹H NMR (400 MHz, DMSO-*d*₆) δ 7.67 (s, 2H, C₃C₅-Ph-H), 3.37–3.35 (m, 2H), 3.14 (t, *J* = 8.2 Hz, 2H, S-CH₂), 2.06 (s, 6H). HRMS: *m/z* 318.0411 [M + 1]⁺. C₁₅H₁₂ClN₃O₃S (317.0390). HPLC purity: 99.62%.

4-((2-Chloro-5,7-dihydrothieno[3,4-*d*]pyrimidin-4-yl)oxy)-3,5-dimethylbenzonitrile (10b). The synthetic method was similar to that described for IIIA-2 except that the starting material was 2,4-dichloro-5,7-dihydrothieno[3,4-*d*]pyrimidine (9b). Recrystallized from EA/PE as a white solid, 88% yield. Mp: 268–270 °C. ¹H NMR (400 MHz, DMSO-*d*₆) δ 7.72 (s, 2H, C₃C₅-Ph-H), 4.12 (s, 2H, S-CH₂), 4.07 (s, 2H, S-CH₂), 2.10 (s, 6H). ESI-MS: *m/z* 318.2 [M + 1]⁺. C₁₅H₁₂ClN₃O₃S (317.04). HPLC purity: 99.20%.

4-((2-Chloro-5,7-dihydrofuro[3,4-*d*]pyrimidin-4-yl)oxy)-3,5-dimethylbenzonitrile (10c). The synthetic method was similar to that described for IIIA-2 except that the starting material was 2,4-dichloro-5,7-dihydrofuro[3,4-*d*]pyrimidine (9c). Recrystallized from EA/PE as a white solid, 88% yield. Mp: 180–183 °C. ¹H NMR (400 MHz, DMSO-*d*₆) δ 7.69 (s, 2H, C₃C₅-Ph-H), 4.97 (s, 2H, C₅-dihydrofuro[3,4-*d*]pyrimidine), 4.80 (s, 2H, C₇-dihydrofuro[3,4-*d*]pyrimidine), 2.10 (s, 6H). HRMS: *m/z* 302.0687 [M + 1]⁺. C₁₅H₁₂ClN₃O₂ (301.0618). HPLC purity: 98.96%.

4-((2-Chloro-6,7-dihydro-5H-cyclopenta[*d*]pyrimidin-4-yl)oxy)-3,5-dimethylbenzonitrile (10d). The synthetic method was similar to that described for IIIA-2 except that the starting material was 2,4-dichloro-6,7-dihydro-5H-cyclopenta[*d*]pyrimidine (9d). Recrystallized from EA/PE as a white solid, 97% yield. Mp: 254–256 °C. ¹H NMR (400 MHz, DMSO-*d*₆) δ 7.73 (s, 2H, C₃C₅-Ph-H), 3.04 (t, *J* = 7.8 Hz, 2H), 2.92 (t, *J* = 7.7 Hz, 2H), 2.13 (p, *J* = 7.7 Hz, 2H), 2.09 (s, 6H). HRMS: *m/z* 300.0895 [M + 1]⁺. C₁₆H₁₄ClN₃O (299.0825). HPLC purity: 99.20%.

4-((2-Chloro-5,6,7,8-tetrahydroquinazolin-4-yl)oxy)-3,5-dimethylbenzonitrile (10e). The synthetic method was similar to that described for IIIA-2 except that the starting material was 2,4-dichloro-5,6,7,8-tetrahydroquinazolin-4-yl (9e). Recrystallized from EA/PE as a white solid, 88% yield. Mp: 175–177 °C. ¹H NMR (400 MHz,

DMSO- d_6) δ 7.65 (s, 2H, C₃,C₅-Ph-H), 2.56 (d, J = 16.0 Hz, 4H), 2.06 (s, 6H), 1.72 (t, J = 3.3 Hz, 4H). HRMS: m/z 314.1053 [M + 1]⁺. C₁₇H₁₆ClN₃O (313.0982). HPLC purity: 98.65%.

4-((2-Chloro-7,8-dihydro-6H-thiopyrano[3,2-d]pyrimidin-4-yl)oxy)-3,5-dimethylbenzonitrile (10f). The synthetic method was similar to that described for IIIA-2 except that the starting material was 2,4-dichloro-7,8-dihydro-6H-thiopyrano[3,2-d]pyrimidine (9f). Recrystallized from EA/PE as a white solid, 66% yield. Mp: 254–255 °C. ¹H NMR (400 MHz, DMSO- d_6) δ : 7.73 (s, 2H), 3.16 (d, J = 5.6 Hz, 2H), 2.92 (t, J = 6.2 Hz, 2H), 2.23–2.13 (m, 2H), 2.07 (s, 6H). ESI-MS: m/z 332.4 [M + 1]⁺. HPLC purity: 98.14%.

General Procedure for the Preparation of Compounds 12a–f. The synthetic method was similar to that described for 7a except that the starting material 10a–f (1.0 mmol) was reacted with *tert*-butyl 4-aminopiperidine-1-carboxylate (1.2 mmol), respectively.

3,5-Dimethyl-4-((2-(piperidin-4-ylamino)-6,7-dihydrothieno[3,2-d]pyrimidin-4-yl)oxy)benzonitrile (12a). Recrystallized from EA/PE as a white solid, 58% yield. Mp: 135–137 °C. ¹H NMR (400 MHz, DMSO- d_6) δ 7.67 (s, 2H, C₃,C₅-Ph-H), 7.09 (s, 1H, NH), 3.36–3.35 (m, 3H), 3.13 (t, J = 8.0 Hz, 2H, S-CH₂), 2.71–2.62 (m, 2H), 2.06 (s, 6H), 1.83–1.45 (m, 6H). HRMS: m/z 382.1692 [M + 1]⁺. C₂₀H₂₃N₅OS (381.1623). HPLC purity: 95.82%.

3,5-Dimethyl-4-((2-(piperidin-4-ylamino)-5,7-dihydrothieno[3,4-d]pyrimidin-4-yl)oxy)benzonitrile (12b). Recrystallized from EA/PE as a white solid, 96% yield. Mp: 268–270 °C. ¹H NMR (400 MHz, DMSO- d_6) δ : 7.72 (s, 2H, C₃,C₅-Ph-H), 6.89 (s, 1H, NH), 4.12 (s, 2H, S-CH₂), 4.08 (s, 2H, S-CH₂), 3.72–3.70 (m, 1H), 2.74–2.72 (m, 2H), 2.10 (s, 6H), 1.97–1.75 (m, 4H), 1.47–1.42 (m, 2H). ESI-MS: m/z 382.2 [M + 1]⁺. C₂₀H₂₃N₅OS (381.16). HPLC purity: 99.47%.

3,5-Dimethyl-4-((2-(piperidin-4-ylamino)-5,7-dihydrofuro[3,4-d]pyrimidin-4-yl)oxy)benzonitrile (12c). Recrystallized from EA/PE as a white solid, 61% yield. Mp: 122–124 °C. ¹H NMR (400 MHz, DMSO- d_6) δ 7.67 (s, 2H, C₃,C₅-Ph-H), 7.08 (s, 1H, NH), 4.96 (s, 2H, C₅-dihydrofuro-pyrimidine), 4.77 (s, 2H, C₇-dihydrofuro-pyrimidine), 3.63–3.61 (m, 1H), 2.67 (s, 2H), 2.09 (s, 6H), 1.97–1.32 (m, 6H). HRMS: m/z 366.1843 [M + 1]⁺. C₂₀H₂₃N₅O₂ (365.1852). HPLC purity: 96.12%.

3,5-Dimethyl-4-((2-(piperidin-4-ylamino)-6,7-dihydro-5H-cyclopenta[d]pyrimidin-4-yl)oxy)benzonitrile (12d). Recrystallized from EA/PE as a white solid, 67% yield. Mp: 135–137 °C. ¹H NMR (400 MHz, DMSO- d_6) δ 7.64 (s, 2H, C₃,C₅-Ph-H), 6.90 (s, 1H, NH), 3.65 (s, 1H), 2.76–2.72 (m, 4H), 2.69–2.59 (m, 2H), 2.07 (s, 6H), 2.02–1.97 (m, 2H), 1.81–1.21 (m, 6H). HRMS: m/z 364.2132 [M + 1]⁺. C₂₁H₂₅N₅O (363.2059). HPLC purity: 95.78%.

3,5-Dimethyl-4-((2-(piperidin-4-ylamino)-5,6,7,8-tetrahydroquinazolin-4-yl)oxy)benzonitrile (12e). Recrystallized from EA/PE as a white solid, 59% yield. Mp: 193–196 °C. ¹H NMR (400 MHz, DMSO- d_6) δ 7.65 (s, 2H, C₃,C₅-Ph-H), 6.82 (s, 1H, NH), 3.59 (s, 1H), 2.72–2.70 (m, 2H), 2.57 (d, J = 16.0 Hz, 4H), 2.06 (s, 6H), 1.76 (t, J = 3.3 Hz, 4H), 1.70–1.23 (m, 6H). HRMS: m/z 378.2283 [M + 1]⁺. C₂₂H₂₇N₅O (377.2216). HPLC purity: 97.14%.

3,5-Dimethyl-4-((2-(piperidin-4-ylamino)-7,8-dihydro-6H-thiopyrano[3,2-d]pyrimidin-4-yl)oxy)benzonitrile (12f). Recrystallized from EA/PE as a white solid, 62% yield. Mp: >250 °C. ESI-MS: m/z 396.4 [M + 1]⁺. C₂₁H₂₅N₅O (395.1780). HPLC purity: 97.93%.

General Procedure for the Preparation of Final Compounds 13a1–6, 13b1–6, 13c1–6, 13d1–6, 13e1–6, and 13f1–6. The synthetic method was similar to that described for 8a1–5 except that the starting material 12a–f (1.0 mmol) was reacted with substituted benzyl chloride (bromide) (1.2 mmol), respectively.

4-((4-((4-(4-Cyano-2,6-dimethylphenoxy)-6,7-dihydrothieno[3,2-d]pyrimidin-2-yl)amino)piperidin-1-yl)methyl)benzenesulfonamide (13a1). Recrystallized from EA/PE as a white solid, 58% yield. Mp: 201–203 °C. ¹H NMR (400 MHz, DMSO- d_6) δ 7.77 (d, J = 8.0 Hz, 2H, C₃,C₅-Ph'-H), 7.67 (s, 2H, C₃,C₅-Ph''-H), 7.45 (d, J = 8.0 Hz, 2H, C₂,C₆-Ph'-H), 7.31 (s, 2H, SO₂NH₂), 7.09 (s, 1H, NH), 3.45 (s, 2H, N-CH₂), 3.37–3.35 (m, 3H), 3.14 (t, J = 8.2 Hz, 2H, S-CH₂), 2.71–2.60 (m, 2H), 2.06 (s, 6H), 1.80–1.20 (m, 6H). ¹³C NMR (100 MHz, DMSO- d_6) δ 162.0, 160.6, 143.3, 143.1, 133.1, 129.4, 126.0, 119.1, 108.6, 61.9, 52.6, 31.5, 29.3, 16.2. HRMS: m/z 551.1890 [M + 1]⁺. C₂₇H₃₀N₆O₃S₂ (550.1821). HPLC purity: 99.71%.

4-((4-((4-(4-Cyano-2,6-dimethylphenoxy)-6,7-dihydrothieno[3,2-d]pyrimidin-2-yl)amino)piperidin-1-yl)methyl)benzamide (13a2). Recrystallized from EA/PE as a white solid, 67% yield. Mp: 245–248 °C. ¹H NMR (400 MHz, DMSO- d_6) δ 7.92 (s, 1H), 7.82 (d, J = 8.0 Hz, 2H, C₃,C₅-Ph'-H), 7.67 (s, 2H, C₃,C₅-Ph''-H), 7.34–7.32 (m, 3H), 6.95 (s, 1H, NH), 3.43 (s, 2H, N-CH₂), 3.39–3.30 (m, 3H), 3.14 (t, J = 8.1 Hz, 2H, S-CH₂), 2.67 (s, 2H), 2.06 (s, 6H), 1.78–1.19 (m, 6H). ¹³C NMR (101 MHz, DMSO- d_6) δ 168.2, 160.6, 142.5, 133.4, 133.1, 132.6, 128.8, 127.8, 108.6, 62.2, 52.6, 36.9, 31.5, 29.3, 16.2. HRMS: m/z 515.2219 [M + 1]⁺. C₂₈H₃₀N₆O₂S (514.2151). HPLC purity: 96.63%.

3,5-Dimethyl-4-((2-((1-(4-(methylsulfonyl)benzyl)piperidin-4-yl)amino)-6,7-dihydrothieno[3,2-d]pyrimidin-4-yl)oxy)benzonitrile (13a3). Recrystallized from EA/PE as a white solid, 70% yield. Mp: 142–144 °C. ¹H NMR (400 MHz, DMSO- d_6) δ 7.87 (d, J = 7.9 Hz, 2H, C₃,C₅-Ph'-H), 7.67 (s, 2H, C₃,C₅-Ph''-H), 7.54 (d, J = 8.0 Hz, 2H, C₂,C₆-Ph'-H), 7.10 (s, 1H, NH), 3.50 (s, 2H, N-CH₂), 3.40–3.29 (m, 3H), 3.20 (s, 3H, SO₂CH₃), 3.15 (t, J = 8.0 Hz, 2H, S-CH₂), 2.67 (s, 2H), 2.07 (s, 6H), 1.77–1.21 (m, 6H). ¹³C NMR (100 MHz, DMSO- d_6) δ 160.6, 145.4, 139.8, 133.1, 132.7, 129.7, 127.4, 119.1, 108.6, 61.8, 52.6, 44.0, 31.6, 29.3, 16.2. HRMS: m/z 550.1946 [M + 1]⁺. C₂₈H₃₁N₅O₃S₂ (549.1868). HPLC purity: 97.62%.

3,5-Dimethyl-4-((2-((1-(pyridin-4-ylmethyl)piperidin-4-yl)amino)-6,7-dihydrothieno[3,2-d]pyrimidin-4-yl)oxy)benzonitrile (13a4). Recrystallized from EA/PE as a white solid, 54% yield. Mp: 140–142 °C. ¹H NMR (400 MHz, DMSO- d_6) δ 8.49 (d, J = 5.4 Hz, 2H, C₃,C₅-Ph'-H), 7.66 (s, 2H, C₃,C₅-Ph''-H), 7.28 (d, J = 5.1 Hz, 2H, C₂,C₆-Ph'), 7.07 (s, 1H, NH), 3.43 (s, 2H, N-CH₂), 3.39–3.25 (m, 3H), 3.15 (t, J = 8.1 Hz, 2H, S-CH₂), 2.67 (s, 2H), 2.07 (s, 6H), 1.79–1.23 (m, 6H). ¹³C NMR (100 MHz, DMSO- d_6) δ 162.0, 160.6, 153.9, 149.9, 148.1, 133.1, 132.6, 124.1, 108.6, 61.2, 52.6, 36.9, 31.5, 29.3, 16.2. HRMS: m/z 473.2118 [M + 1]⁺. C₂₆H₂₈N₆O (472.2045). HPLC purity: 99.33%.

3,5-Dimethyl-4-((2-((1-(4-nitrobenzyl)piperidin-4-yl)amino)-6,7-dihydrothieno[3,2-d]pyrimidin-4-yl)oxy)benzonitrile (13a5). Recrystallized from EA/PE as a white solid, 62% yield. Mp: 158–160 °C. ¹H NMR (400 MHz, DMSO- d_6) δ 8.19 (d, J = 8.3 Hz, 2H, C₃,C₅-Ph'-H), 7.66 (s, 2H, C₃,C₅-Ph''-H), 7.55 (d, J = 8.3 Hz, 2H, C₂,C₆-Ph'-H), 7.07 (s, 1H, NH), 3.54 (s, 2H, N-CH₂), 3.39–3.25 (m, 3H), 3.15 (t, J = 8.0 Hz, 2H, S-CH₂), 2.68 (s, 2H), 2.07 (s, 6H), 1.82–1.20 (m, 6H). ¹³C NMR (100 MHz, DMSO- d_6) δ 162.0, 160.6, 147.5, 146.9, 133.1, 132.7, 130.0, 123.8, 119.0, 108.6, 61.6, 52.6, 39.4, 36.9, 31.6, 29.3, 16.2. HRMS: m/z 517.2016 [M + 1]⁺. C₂₇H₂₈N₆O₃S (516.1944). HPLC purity: 99.92%.

3-((4-((4-(4-Cyano-2,6-dimethylphenoxy)-6,7-dihydrothieno[3,2-d]pyrimidin-2-yl)amino)piperidin-1-yl)methyl)benzamide (13a6). Recrystallized from EA/PE as a white solid, 47% yield. Mp: 215–217 °C. ¹H NMR (400 MHz, DMSO- d_6) δ 7.95 (s, 1H, C₂-Ph'-H), 7.75 (dd, J = 11.0, 3.9 Hz, 2H, C₅,C₆-Ph'-H), 7.66 (s, 2H, C₃,C₅-Ph''-H), 7.46–7.25 (m, 3H), 7.06 (s, 1H, NH), 3.43 (s, 2H, N-CH₂), 3.39–3.25 (m, 3H), 3.15 (t, J = 8.1 Hz, 2H, S-CH₂), 2.68 (s, 2H), 2.07 (s, 6H), 1.81–1.24 (m, 6H). ¹³C NMR (100 MHz, DMSO- d_6) δ 168.4, 162.0, 160.6, 139.2, 134.6, 133.1, 132.7, 132.0, 128.4, 126.4, 119.0, 108.6, 62.4, 52.6, 36.9, 31.6, 29.3, 16.2. HRMS: m/z 515.2229 [M + 1]⁺. C₂₈H₃₀N₆O₂S (514.2151). HPLC purity: 99.95%.

4-((4-((4-(4-Cyano-2,6-dimethylphenoxy)-5,7-dihydrothieno[3,4-d]pyrimidin-2-yl)amino)piperidin-1-yl)methyl)benzenesulfonamide (13b1). Recrystallized from EA/PE as a white solid, 79% yield. Mp: 144–146 °C. ¹H NMR (400 MHz, DMSO- d_6) δ 7.78 (d, J = 8.2 Hz, 2H, C₃,C₅-Ph'-H), 7.72 (s, 2H, C₃,C₅-Ph''-H), 7.46 (d, J = 8.1 Hz, 2H, C₂,C₆-Ph'-H), 7.30 (s, 2H, SO₂NH₂), 6.89 (s, 1H, NH), 4.12 (s, 2H, S-CH₂), 4.08 (s, 2H, S-CH₂), 3.72 (s, 1H), 3.42 (s, 2H, N-CH₂), 2.72–2.74 (m, 2H), 2.10 (s, 6H), 1.79–2.04 (m, 4H), 1.41–1.47 (m, 2H). ¹³C NMR (100 MHz, DMSO- d_6) δ 165.7, 161.7, 160.3, 153.7, 143.0, 135.3, 134.2, 126.0, 123.9, 123.7, 119.2, 109.7, 61.2, 52.8, 48.3, 31.7, 16.2. HRMS: m/z 551.1890 [M + 1]⁺. C₂₇H₃₀N₆O₃S₂ (550.1821). HPLC purity: 98.77%.

3,5-Dimethyl-4-((2-((1-(4-(methylsulfonyl)benzyl)piperidin-4-yl)amino)-5,7-dihydrothieno[3,4-d]pyrimidin-4-yl)oxy)benzonitrile (13b2). Recrystallized from EA/PE as a white solid, 79% yield. Mp: 144–146 °C. ¹H NMR (400 MHz, DMSO- d_6) δ 7.78 (d, J = 8.2 Hz, 2H, C₃,C₅-Ph'-H), 7.72 (s, 2H, C₃,C₅-Ph''-H), 7.46 (d, J = 8.1 Hz, 2H, C₂,C₆-Ph'-H), 7.30 (s, 2H, SO₂NH₂), 6.89 (s, 1H, NH), 4.12 (s, 2H, S-CH₂), 4.08 (s, 2H, S-CH₂), 3.72 (s, 1H), 3.42 (s, 2H, N-CH₂), 2.72–2.74 (m, 2H), 2.10 (s, 6H), 1.79–2.04 (m, 4H), 1.41–1.47 (m, 2H). ¹³C NMR (100 MHz, DMSO- d_6) δ 165.7, 161.7, 160.3, 153.7, 143.0, 135.3, 134.2, 126.0, 123.9, 123.7, 119.2, 109.7, 61.2, 52.8, 48.3, 31.7, 16.2. HRMS: m/z 551.1890 [M + 1]⁺. C₂₇H₃₀N₆O₃S₂ (550.1821). HPLC purity: 98.77%.

benzoxazole (13b2). Recrystallized from EA/PE as a white solid, 71% yield. Mp: 181–183 °C. ¹H NMR (400 MHz, DMSO-*d*₆, ppm): δ 7.84 (d, 2H, *J* = 8.2 Hz, C₃,C₅-Ph'-H), 7.71 (s, 2H, C₃,C₅-Ph''-H), 7.52 (d, 2H, *J* = 8.2 Hz, C₂,C₆-Ph'-H), 6.88 (s, 1H, NH), 4.12 (s, 2H, S-CH₂), 4.08 (s, 2H, S-CH₂), 3.75–3.78 (m, 1H), 3.57 (s, 2H, N-CH₂), 3.06 (s, 3H, SO₂CH₃), 2.71–2.75 (m, 2H), 2.10 (s, 6H), 1.96–2.09 (m, 4H), 1.39–1.41 (m, 2H). ¹³C NMR (100 MHz, DMSO-*d*₆): δ 165.1, 162.3, 159.4, 153.9, 145.2, 139.5, 134.3, 133.0, 126.8, 123.3, 118.9, 109.7, 62.3, 52.6, 48.5, 44.7, 32.0, 16.6. HRMS: *m/z* 550.1942 [M + 1]⁺. C₂₈H₃₁N₅O₃S₂ (549.1868). HPLC purity: 95.16%.

3,5-Dimethyl-4-((2-((1-(4-nitrobenzyl)piperidin-4-yl)amino)-5,7-dihydrothieno[3,4-*d*]pyrimidin-4-yl)oxy)benzoxazole (13b3). Recrystallized from EA/PE as a white solid, 82% yield. Mp: 180–182 °C. ¹H NMR (400 MHz, DMSO-*d*₆, ppm): δ 7.84 (d, 2H, *J* = 8.3 Hz, C₃,C₅-Ph'-H), 7.72 (s, 2H, C₃,C₅-Ph''-H), 7.57 (d, *J* = 8.4 Hz, 2H, C₂,C₆-Ph'-H), 6.90 (s, 1H, NH), 4.14 (s, 2H, S-CH₂), 4.05 (s, 2H, S-CH₂), 3.75–3.76 (m, 1H), 3.59 (s, 2H, N-CH₂), 2.73–2.75 (m, 2H), 2.11 (s, 6H), 1.80–1.85 (m, 2H), 1.41–1.44 (m, 4H). ¹³C NMR (100 MHz, DMSO-*d*₆): δ 162.8, 160.7, 153.0, 147.6, 147.1, 141.3, 136.4, 133.7, 132.9, 123.8, 119.3, 109.8, 61.6, 52.9, 48.2, 31.7, 16.2. HRMS: *m/z* 517.2015 [M + 1]⁺. C₂₇H₂₈N₆O₃S (516.1944). HPLC purity: 95.28%.

4-((2-((1-(4-Aminobenzyl)piperidin-4-yl)amino)-5,7-dihydrothieno[3,4-*d*]pyrimidin-4-yl)oxy)-3,5-dimethylbenzoxazole (13b4). Recrystallized from EA/PE as a white solid, 55% yield. Mp: 143–145 °C. ¹H NMR (400 MHz, DMSO-*d*₆, ppm): δ 7.80 (d, 2H, *J* = 8.3 Hz, C₃,C₅-Ph'-H), 7.71 (s, 2H, C₃,C₅-Ph''-H), 7.54 (d, *J* = 8.4 Hz, 2H, C₂,C₆-Ph'-H), 6.92 (s, 1H, NH), 4.83 (s, 2H, NH₂), 4.12 (s, 2H, S-CH₂), 4.04 (s, 2H, S-CH₂), 3.73–3.76 (m, 1H), 3.58 (s, 2H, N-CH₂), 2.71–2.73 (m, 2H), 2.10 (s, 6H), 1.82–1.87 (m, 2H), 1.71–1.73 (m, 2H), 1.45–1.48 (m, 2H). ¹³C NMR (100 MHz, DMSO-*d*₆): δ 162.0, 160.7, 153.1, 147.3, 146.7, 140.3, 136.9, 133.4, 132.2, 123.1, 119.3, 109.5, 61.6, 52.4, 48.5, 31.7, 16.2. HRMS: *m/z* 487.2272 [M + 1]⁺. C₂₇H₃₀N₆O₃S (486.2202). HPLC purity: 96.38%.

N-(4-((4-((4-(4-Cyano-2,6-dimethylphenoxy)-5,7-dihydrothieno[3,4-*d*]pyrimidin-2-yl)amino)piperidin-1-yl)methyl)phenyl)methanesulfonamide (13b5). Recrystallized from EA/PE as a white solid, 47% yield. Mp: 186–187 °C. ¹H NMR (400 MHz, DMSO-*d*₆) δ: 9.68 (s, 1H), 7.67 (s, 2H, C₃,C₅-Ph''-H), 7.20 (d, *J* = 8.2 Hz, 2H, C₃,C₅-Ph'-H), 7.13 (d, *J* = 8.1 Hz, 2H, C₂,C₆-Ph'-H), 6.97 (s, 1H), 4.13 (s, 2H, S-CH₂), 4.07 (s, 2H, S-CH₂), 3.66 (s, 1H), 3.35 (s, 2H, N-CH₂), 2.96 (s, 3H, SO₂CH₃), 2.63–2.73 (m, 2H), 2.08 (s, 6H, 2 × CH₃), 1.23–1.89 (m, 6H). ¹³C NMR (100 MHz, DMSO) δ: 164.4, 162.1, 153.7, 151.0, 137.5, 133.1, 132.5, 130.1, 120.4, 120.2, 119.1, 116.1, 113.4, 112.2, 108.6, 93.6, 62.0, 52.3, 48.4, 31.6, 16.3. HRMS: *m/z* 566.2133 [M + 1]⁺. C₂₈H₃₂N₆O₃S₂ (564.1977). HPLC purity: 98.01%.

4-((4-((4-(4-Cyano-2,6-dimethylphenoxy)-5,7-dihydrofuro[3,4-*d*]pyrimidin-2-yl)amino)piperidin-1-yl)methyl)benzenesulfonamide (13c1). Recrystallized from EA/PE as a white solid, 66% yield. Mp: 191–193 °C. ¹H NMR (400 MHz, DMSO-*d*₆) δ 7.77 (d, *J* = 8.0 Hz, 2H, C₃,C₅-Ph'-H), 7.67 (s, 2H, C₃,C₅-Ph''-H), 7.45 (d, *J* = 8.0 Hz, 2H, C₂,C₆-Ph'-H), 7.31 (s, 2H, SO₂NH₂), 7.08 (s, 1H, NH), 4.96 (s, 2H, C₅-dihydrofurofuryrimidine), 4.77 (s, 2H, C₇-dihydrofurofuryrimidine), 3.63 (s, 1H), 3.47 (s, 2H, N-CH₂), 2.69 (s, 2H), 2.09 (s, 6H), 1.94–1.18 (m, 6H). ¹³C NMR (100 MHz, DMSO-*d*₆) δ 162.9, 162.0, 143.3, 143.1, 133.1, 129.4, 126.9, 126.2, 126.0, 119.0, 61.9, 52.6, 31.5, 16.2. HRMS: *m/z* 535.2126 [M + 1]⁺. C₂₇H₃₀N₆O₄S (534.2049). HPLC purity: 97.68%.

4-((4-((4-(4-Cyano-2,6-dimethylphenoxy)-5,7-dihydrofuro[3,4-*d*]pyrimidin-2-yl)amino)piperidin-1-yl)methyl)benzamide (13c2). Recrystallized from EA/PE as a white solid, 57% yield. Mp: 238–240 °C. ¹H NMR (400 MHz, DMSO-*d*₆) δ 7.85 (s, 2H, CONH₂), 7.75 (d, *J* = 7.9 Hz, 2H, C₃,C₅-Ph'-H), 7.60 (s, 2H, C₃,C₅-Ph''-H), 7.26 (d, *J* = 8.1 Hz, 2H, C₂,C₆-Ph'-H), 7.00 (s, 1H, NH), 4.89 (s, 2H, C₅-dihydrofurofuryrimidine), 4.70 (s, 2H, C₇-dihydrofurofuryrimidine), 3.60 (s, 1H), 3.42 (s, 2H, N-CH₂), 2.74–2.53 (m, 2H), 2.02 (s, 6H), 1.93–1.11 (m, 6H). ¹³C NMR (100 MHz, DMSO-*d*₆) δ 168.2, 162.9, 162.5, 142.5, 133.4, 133.1, 132.5, 128.8, 127.8, 119.0, 108.7, 62.2, 52.6, 31.6, 16.2. HRMS: *m/z* 499.2457 [M + 1]⁺. C₂₈H₃₀N₆O₃ (498.2397). HPLC purity: 99.27%.

3,5-Dimethyl-4-((2-((1-(4-(methylsulfonyl)benzyl)piperidin-4-yl)amino)-5,7-dihydrofuro[3,4-*d*]pyrimidin-4-yl)oxy)benzoxazole (13c3). Recrystallized from EA/PE as a white solid, 72% yield. Mp: 209–211 °C. ¹H NMR (400 MHz, DMSO-*d*₆) δ 7.87 (d, *J* = 8.0 Hz, 2H, C₃,C₅-Ph'-H), 7.67 (s, 2H, C₃,C₅-Ph''-H), 7.54 (d, *J* = 8.0 Hz, 2H, C₂,C₆-Ph'-H), 7.08 (s, 1H, NH), 4.96 (s, 2H, C₅-dihydrofurofuryrimidine), 4.77 (s, 2H, C₇-dihydrofurofuryrimidine), 3.68 (s, 1H), 3.51 (s, 2H, N-CH₂), 3.20 (s, 3H, SO₂CH₃), 2.76–2.62 (m, 2H), 2.09 (s, 6H), 1.90–1.15 (m, 6H). ¹³C NMR (100 MHz, DMSO-*d*₆) δ 162.9, 162.5, 145.4, 139.8, 133.1, 129.7, 127.4, 108.7, 69.3, 61.8, 52.6, 44.0, 31.5, 16.2. HRMS: *m/z* 534.2173 [M + 1]⁺. C₂₈H₃₁N₅O₄S (533.2097). HPLC purity: 99.34%.

3,5-Dimethyl-4-((2-((1-(pyridin-4-ylmethyl)piperidin-4-yl)amino)-5,7-dihydrofuro[3,4-*d*]pyrimidin-4-yl)oxy)benzoxazole (13c4). Recrystallized from EA/PE as a white solid, 73% yield. Mp: 155–157 °C. ¹H NMR (400 MHz, DMSO-*d*₆) δ 8.50 (d, *J* = 5.9 Hz, 2H, C₃,C₅-Ph'-H), 7.67 (s, 2H, C₃,C₅-Ph''-H), 7.28 (d, *J* = 5.1 Hz, 2H, C₂,C₆-Ph'-H), 7.09 (s, 1H, NH), 4.96 (s, 2H, C₅-dihydrofurofuryrimidine), 4.77 (s, 2H, C₇-dihydrofurofuryrimidine), 3.68 (s, 1H), 3.45 (s, 2H, N-CH₂), 2.77–2.59 (m, 2H), 2.09 (s, 6H), 1.91–1.22 (m, 6H). ¹³C NMR (100 MHz, DMSO-*d*₆) δ 162.9, 149.9, 148.1, 133.1, 124.1, 108.7, 69.4, 61.2, 52.6, 31.4, 16.2. HRMS: *m/z* 457.2345 [M + 1]⁺. C₂₆H₂₈N₆O₂ (456.2274). HPLC purity: 97.81%.

3,5-Dimethyl-4-((2-((1-(4-nitrobenzyl)piperidin-4-yl)amino)-5,7-dihydrofuro[3,4-*d*]pyrimidin-4-yl)oxy)benzoxazole (13c5). Recrystallized from EA/PE as a white solid, 61% yield. Mp: 199–201 °C. ¹H NMR (400 MHz, DMSO-*d*₆) δ 8.12 (d, *J* = 8.6 Hz, 2H, C₃,C₅-Ph'-H), 7.60 (s, 2H, C₃,C₅-Ph''-H), 7.49 (d, *J* = 8.4 Hz, 2H, C₂,C₆-Ph'-H), 7.02 (s, 1H, NH), 4.89 (s, 2H, C₅-dihydrofurofuryrimidine), 4.70 (s, 2H, C₇-dihydrofurofuryrimidine), 3.61 (s, 1H), 3.47 (s, 2H, N-CH₂), 2.63 (s, 2H), 2.02 (s, 6H), 1.80–1.14 (m, 6H). ¹³C NMR (100 MHz, DMSO-*d*₆) δ 162.9, 146.9, 133.1, 130.0, 123.8, 61.6, 52.6, 39.6, 39.4, 31.5, 16.2. HRMS: *m/z* 501.2247 [M + 1]⁺. C₂₇H₂₈N₆O₄ (500.2172). HPLC purity: 95.77%.

3-((4-((4-(4-Cyano-2,6-dimethylphenoxy)-5,7-dihydrofuro[3,4-*d*]pyrimidin-2-yl)amino)piperidin-1-yl)methyl)benzamide (13c6). Recrystallized from EA/PE as a white solid, 43% yield. Mp: 225–227 °C. ¹H NMR (400 MHz, DMSO-*d*₆) δ 7.88 (s, 2H, CONH₂), 7.70 (s, 1H, C₂-Ph'-H), 7.69–7.66 (m, 1H), 7.60 (s, 2H, C₃,C₅-Ph''-H), 7.35–7.30 (m, 2H, C₂,C₆-Ph'-H), 7.01 (s, 1H, NH), 4.89 (s, 2H, C₅-dihydrofurofuryrimidine), 4.70 (s, 2H, C₇-dihydrofurofuryrimidine), 3.60 (s, 1H), 3.36 (s, 2H, N-CH₂), 2.63 (s, 2H), 2.02 (s, 6H), 1.92–1.16 (m, 6H). ¹³C NMR (100 MHz, DMSO-*d*₆) δ 168.4, 163.0, 162.5, 139.2, 134.6, 133.1, 132.0, 128.4, 126.4, 119.0, 108.7, 69.4, 62.4, 55.3, 52.6, 39.6, 31.6, 16.2. HRMS: *m/z* 499.2456 [M + 1]⁺. C₂₈H₃₀N₆O₃ (498.2379). HPLC purity: 97.74%.

4-((4-((4-(4-Cyano-2,6-dimethylphenoxy)-6,7-dihydro-5H-cyclopenta[*d*]pyrimidin-2-yl)amino)piperidin-1-yl)methyl)benzenesulfonamide (13d1). Recrystallized from EA/PE as a white solid, 80% yield. Mp: 207–209 °C. ¹H NMR (400 MHz, DMSO-*d*₆) δ 7.77 (d, *J* = 8.3 Hz, 2H, C₃,C₅-Ph'-H), 7.64 (s, 2H, C₃,C₅-Ph''-H), 7.45 (d, *J* = 8.1 Hz, 2H, C₂,C₆-Ph'-H), 7.30 (s, 2H, SO₂NH₂), 6.90 (s, 1H, NH), 3.65 (s, 1H), 3.45 (s, 2H), 2.76 (dt, *J* = 22.3, 7.7 Hz, 4H), 2.69–2.59 (m, 2H), 2.07 (s, 6H), 2.02 (d, *J* = 7.4 Hz, 2H), 1.81–1.21 (m, 6H). ¹³C NMR (100 MHz, DMSO-*d*₆) δ 162.0, 143.3, 143.1, 133.1, 132.6, 129.4, 126.0, 119.1, 108.3, 62.0, 52.6, 39.6, 31.6, 25.9, 22.0, 16.3. HRMS: *m/z* 533.2330 [M + 1]⁺. C₂₈H₃₂N₆O₃S (532.2257). HPLC purity: 97.64%.

4-((4-((4-(4-Cyano-2,6-dimethylphenoxy)-6,7-dihydro-5H-cyclopenta[*d*]pyrimidin-2-yl)amino)piperidin-1-yl)methyl)benzamide (13d2). Recrystallized from EA/PE as a white solid, 68% yield. Mp: 225–227 °C. ¹H NMR (400 MHz, DMSO-*d*₆) δ 7.90 (s, 2H, CONH₂), 7.81 (d, *J* = 7.9 Hz, 2H, C₃,C₅-Ph'-H), 7.64 (s, 2H, C₃,C₅-Ph''-H), 7.32 (d, *J* = 8.0 Hz, 2H, C₂,C₆-Ph'-H), 6.89 (s, 1H, NH), 3.65 (s, 1H), 3.48–3.36 (m, 2H), 2.76 (dt, *J* = 22.1, 7.7 Hz, 4H), 2.70–2.58 (m, 2H), 2.07 (s, 6H), 2.02 (d, *J* = 7.4 Hz, 2H), 1.70–1.23 (m, 6H). ¹³C NMR (100 MHz, DMSO-*d*₆) δ 168.2, 162.0, 143.1, 142.5, 133.4, 133.1, 129.5, 128.8, 127.8, 119.5, 108.9, 62.2, 52.7, 39.0, 31.2, 25.9, 22.0, 16.3. HRMS: *m/z* 497.2657 [M + 1]⁺. C₂₉H₃₂N₆O₂ (496.2587). HPLC purity: 95.88%.

3,5-Dimethyl-4-((2-((1-(4-(methylsulfonyl)benzyl)piperidin-4-yl)amino)-6,7-dihydro-5H-cyclopenta[d]pyrimidin-4-yl)oxy)benzimidazole (13d3). Recrystallized from EA/PE as a white solid, 69% yield. Mp: 170–172 °C. ¹H NMR (400 MHz, DMSO-*d*₆) δ 7.89–7.85 (m, 2H), 7.65 (s, 2H, C₃C₅-Ph'-H), 7.54 (d, *J* = 8.1 Hz, 2H), 6.80 (s, 1H, NH), 3.66 (s, 1H), 3.50 (s, 2H, N-CH₂), 2.89 (s, 3H), 2.78 (dd, *J* = 14.7, 7.3 Hz, 4H), 2.71–2.61 (m, 2H), 2.07 (s, 6H), 2.03 (d, *J* = 7.5 Hz, 2H), 1.81–1.23 (m, 6H). ¹³C NMR (100 MHz, DMSO-*d*₆) δ 162.7, 162.0, 145.4, 139.8, 133.1, 132.6, 129.7, 127.4, 127.3, 108.3, 62.6, 61.9, 52.6, 44.1, 44.0, 36.2, 31.6, 31.2, 25.9, 22.0, 16.3. HRMS: *m/z* 532.2377 [M + 1]⁺. C₂₉H₃₃N₅O₃S (531.2304). HPLC purity: 96.53%.

3,5-Dimethyl-4-((2-((1-(pyridin-4-ylmethyl)piperidin-4-yl)amino)-6,7-dihydro-5H-cyclopenta[d]pyrimidin-4-yl)oxy)benzimidazole (13d4). Recrystallized from EA/PE as a white solid, 72% yield. Mp: 173–175 °C. ¹H NMR (400 MHz, DMSO-*d*₆) δ 8.57 (d, *J* = 7.9 Hz, 2H, C₃C₅-Ph'-H), 7.64 (s, 2H, C₃C₅-Ph''-H), 7.28 (d, *J* = 8.0 Hz, 2H, C₂C₆-Ph'-H), 6.83 (s, 1H, NH), 3.60 (s, 1H), 3.48–3.42 (m, 2H), 2.76 (dt, *J* = 21.6, 7.2 Hz, 4H), 2.70–2.62 (m, 2H), 2.07 (s, 6H), 2.02 (d, *J* = 7.4 Hz, 2H), 1.85–1.21 (m, 6H). ¹³C NMR (100 MHz, DMSO-*d*₆) δ 168.2, 162.4, 142.9, 142.1, 133.7, 133.2, 129.5, 127.8, 1120.3, 108.7, 62.2, 52.6, 39.0, 31.6, 25.9, 22.0, 16.3. HRMS: *m/z* 455.2557 [M + 1]⁺. C₂₇H₃₀N₆O (454.2481). HPLC purity: 96.17%.

3,5-Dimethyl-4-((2-((1-(4-nitrobenzyl)piperidin-4-yl)amino)-6,7-dihydro-5H-cyclopenta[d]pyrimidin-4-yl)oxy)benzimidazole (13d5). Recrystallized from EA/PE as a white solid, 71% yield. Mp: 200–212 °C. ¹H NMR (400 MHz, DMSO-*d*₆) δ 8.17 (d, *J* = 8.1 Hz, 2H, C₃C₅-Ph'-H), 7.65 (s, 2H, C₃C₅-Ph''-H), 7.54 (d, *J* = 8.1 Hz, 2H), 6.80 (s, 1H, NH), 3.72 (s, 1H), 3.50 (s, 2H, N-CH₂), 2.78 (dd, *J* = 14.4, 7.2 Hz, 4H), 2.71–2.64 (m, 2H), 2.07 (s, 6H), 2.03 (d, *J* = 7.5 Hz, 2H), 1.81–1.23 (m, 6H). ¹³C NMR (100 MHz, DMSO-*d*₆) δ 159.7, 147.5, 146.9, 145.4, 139.8, 133.1, 132.6, 130.2, 127.4, 123.8, 108.3, 62.1, 61.7, 52.6, 44.1, 36.2, 31.6, 31.2, 25.9, 21.8, 16.2. HRMS: *m/z* 499.2456 [M + 1]⁺. C₂₈H₃₀N₆O₃ (498.2379). HPLC purity: 99.14%.

3-((4-((4-Cyano-2,6-dimethylphenoxy)-6,7-dihydro-5H-cyclopenta[d]pyrimidin-2-yl)amino)piperidin-1-yl)methyl)benzamide (13d6). Recrystallized from EA/PE as a white solid, 59% yield. Mp: 234–236 °C. ¹H NMR (400 MHz, DMSO-*d*₆) δ 7.96 (s, 2H, CONH₂), 7.79–7.75 (m, 1H), 7.65 (s, 2H, C₃C₅-Ph''-H), 7.39–7.35 (m, 3H), 6.80 (s, 1H, NH), 3.72 (s, 1H), 3.50 (s, 2H, N-CH₂), 2.78 (dd, *J* = 14.3, 7.2 Hz, 4H), 2.71–2.63 (m, 2H), 2.07 (s, 6H), 2.03 (d, *J* = 7.5 Hz, 2H), 1.80–1.18 (m, 6H). ¹³C NMR (100 MHz, DMSO-*d*₆) δ 168.2, 162.3, 143.2, 142.5, 133.4, 133.1, 129.4, 128.8, 127.6, 119.5, 108.9, 62.2, 52.7, 39.0, 31.3, 25.9, 22.0, 16.3. ESI-MS: *m/z* 497.2657 [M + 1]⁺. C₂₉H₃₂N₆O₂ (496.2587). HPLC purity: 95.93%.

4-((4-((4-Cyano-2,6-dimethylphenoxy)-5,6,7,8-tetrahydroquinazolin-2-yl)amino)piperidin-1-yl)methyl)benzenesulfonamide (13e1). Recrystallized from EA/PE as a white solid, 63% yield. Mp: 221–224 °C. ¹H NMR (400 MHz, DMSO-*d*₆) δ 7.77 (d, *J* = 8.0 Hz, 2H, C₃C₅-Ph'-H), 7.65 (s, 2H, C₃C₅-Ph''-H), 7.45 (d, *J* = 7.9 Hz, 2H, C₂C₆-Ph'-H), 7.32 (s, 2H, SO₂NH₂), 6.82 (s, 1H, NH), 3.59 (s, 1H), 3.45 (s, 2H, N-CH₂), 2.72–2.69 (m, 2H), 2.57 (d, *J* = 16.0 Hz, 4H), 2.06 (s, 6H), 1.76 (t, *J* = 3.3 Hz, 4H), 1.70–1.01 (m, 6H). ¹³C NMR (100 MHz, DMSO-*d*₆) δ 166.0, 143.3, 143.1, 133.1, 132.5, 129.4, 126.0, 108.2, 62.0, 52.6, 39.4, 31.7, 22.5, 21.3, 16.2. HRMS: *m/z* 547.2485 [M + 1]⁺. C₂₉H₃₄N₆O₃S (546.2413). HPLC purity: 98.01%.

4-((4-((4-Cyano-2,6-dimethylphenoxy)-5,6,7,8-tetrahydroquinazolin-2-yl)amino)piperidin-1-yl)methyl)benzamide (13e2). Recrystallized from EA/PE as a white solid, 62% yield. Mp: 230–232 °C. ¹H NMR (400 MHz, DMSO-*d*₆) δ 7.90 (s, 2H, CONH₂), 7.81 (d, *J* = 7.7 Hz, 2H, C₃C₅-Ph'-H), 7.64 (s, 2H, C₃C₅-Ph''-H), 7.31 (d, *J* = 7.9 Hz, 2H, C₂C₆-Ph'-H), 6.80 (s, 1H, NH), 3.57 (s, 1H), 3.42 (s, 2H, N-CH₂), 2.70–2.69 (m, 2H), 2.57 (d, *J* = 17.9 Hz, 4H), 2.06 (s, 6H), 1.84–1.71 (m, 4H), 1.69–1.12 (m, 6H). ¹³C NMR (100 MHz, DMSO-*d*₆) δ 166.4, 143.7, 143.1, 133.2, 132.5, 130.0, 126.0, 108.3, 62.1, 51.9, 39.9, 31.7, 22.5, 21.3, 16.2. HRMS: *m/z* 511.2816 [M + 1]⁺. C₃₀H₃₄N₆O₂ (510.2743). HPLC purity: 98.81%.

3,5-Dimethyl-4-((2-((1-(4-(methylsulfonyl)benzyl)piperidin-4-yl)amino)-5,6,7,8-tetrahydroquinazolin-4-yl)oxy)benzimidazole (13e3). Recrystallized from EA/PE as a white solid, 62% yield. Mp: 203–206 °C. ¹H NMR (400 MHz, DMSO-*d*₆) δ 7.87 (d, *J* =

7.9 Hz, 2H, C₃C₅-Ph'-H), 7.65 (s, 2H, C₃C₅-Ph''-H), 7.54 (d, *J* = 8.0 Hz, 2H, C₂C₆-Ph'-H), 6.83 (s, 1H, NH), 3.57 (s, 1H), 3.49 (s, 2H, N-CH₂), 3.20 (s, 3H, SO₂CH₃), 2.66 (s, 2H), 2.57 (d, *J* = 15.6 Hz, 4H), 2.06 (s, 6H), 1.84–1.71 (m, 4H), 1.70–1.17 (m, 6H). ¹³C NMR (100 MHz, DMSO-*d*₆) δ 166.0, 145.4, 139.7, 133.1, 132.6, 129.7, 127.4, 61.9, 52.6, 44.0, 31.7, 22.5, 21.3, 16.2. HRMS: *m/z* 546.2530 [M + 1]⁺. C₃₀H₃₅N₅O₃S (545.2461). HPLC purity: 97.14%.

3,5-Dimethyl-4-((2-((1-(pyridin-4-ylmethyl)piperidin-4-yl)amino)-5,6,7,8-tetrahydroquinazolin-4-yl)oxy)benzimidazole (13e4). Recrystallized from EA/PE as a white solid, 51% yield. Mp: 181–184 °C. ¹H NMR (400 MHz, DMSO-*d*₆) δ 8.59 (d, *J* = 8.0 Hz, 2H, C₃C₅-Ph'-H), 7.65 (s, 2H, C₃C₅-Ph''-H), 7.27 (d, *J* = 5.2 Hz, 2H, C₂C₆-Ph'-H), 6.81 (s, 1H, NH), 3.57 (s, 1H), 3.42 (s, 2H, N-CH₂), 2.64 (s, 2H), 2.57 (d, *J* = 15.2 Hz, 4H), 2.06 (s, 6H), 1.76 (p, *J* = 2.9 Hz, 4H), 1.69–1.14 (m, 6H). ¹³C NMR (100 MHz, DMSO-*d*₆) δ 166.0, 159.4, 149.9, 148.1, 133.1, 132.5, 124.0, 61.2, 52.6, 32.0, 31.6, 22.5, 21.3, 16.2. HRMS: *m/z* 469.2710 [M + 1]⁺. C₂₈H₃₂N₆O (468.2638). HPLC purity: 99.89%.

3,5-Dimethyl-4-((2-((1-(4-nitrobenzyl)piperidin-4-yl)amino)-5,6,7,8-tetrahydroquinazolin-4-yl)oxy)benzimidazole (13e5). Recrystallized from EA/PE as a white solid, 49% yield. Mp: 225–227 °C. ¹H NMR (400 MHz, DMSO-*d*₆) δ 8.19 (d, *J* = 8.2 Hz, 2H, C₃C₅-Ph'-H), 7.64 (s, 2H, C₃C₅-Ph''-H), 7.55 (d, *J* = 8.3 Hz, 2H, C₂C₆-Ph'-H), 6.83 (s, 1H, NH), 3.75 (s, 1H), 3.53 (s, 2H, N-CH₂), 2.66 (s, 2H), 2.57 (d, *J* = 15.7 Hz, 4H), 2.06 (s, 6H), 1.86–1.69 (m, 4H), 1.70–1.09 (m, 6H). ¹³C NMR (100 MHz, DMSO-*d*₆) δ 166.0, 147.5, 146.9, 133.1, 132.5, 130.0, 123.8, 108.2, 61.6, 52.6, 31.7, 22.5, 21.3, 16.2. HRMS: *m/z* 513.2605 [M + 1]⁺. C₂₉H₃₂N₆O₃ (512.2536). HPLC purity: 99.51%.

3-((4-((4-Cyano-2,6-dimethylphenoxy)-5,6,7,8-tetrahydroquinazolin-2-yl)amino)piperidin-1-yl)methyl)benzamide (13e6). Recrystallized from EA/PE as a white solid, 57% yield. Mp: 251–253 °C. ¹H NMR (400 MHz, DMSO-*d*₆) δ 7.96 (s, 2H, CONH₂), 7.79–7.72 (m, 1H), 7.65 (s, 2H, C₃C₅-Ph''-H), 7.39–7.36 (m, 3H), 6.80 (s, 1H, NH), 3.61 (s, 1H), 3.42 (s, 2H, N-CH₂), 2.67 (s, 2H), 2.57 (d, *J* = 14.9 Hz, 4H), 2.06 (s, 6H), 1.76 (p, *J* = 3.0 Hz, 4H), 1.70–1.42 (m, 6H). ¹³C NMR (100 MHz, DMSO-*d*₆) δ 168.4, 166.0, 139.2, 134.6, 133.1, 132.6, 132.0, 128.4, 126.4, 62.4, 52.6, 31.7, 22.5, 21.3, 16.2. HRMS: *m/z* 511.2812 [M + 1]⁺. C₃₀H₃₄N₆O₂ (510.2743). HPLC purity: 99.73%.

4-((4-((4-Cyano-2,6-dimethylphenoxy)-7,8-dihydro-6H-thiopyrano[3,2-*d*]pyrimidin-2-yl)amino)piperidin-1-yl)methyl)benzenesulfonamide (13f1). Recrystallized from EA/PE as a white solid, 84% yield. Mp: 193–195 °C. ¹H NMR (400 MHz, DMSO-*d*₆) δ: 7.77 (d, *J* = 8.3 Hz, 2H), 7.66 (s, 2H), 7.45 (d, *J* = 8.0 Hz, 2H), 7.30 (s, 2H), 6.88 (s, 1H), 3.45 (s, 2H), 3.13–2.95 (m, 2H), 2.91–2.57 (m, 4H), 2.16–2.08 (m, 2H), 2.06 (s, 6H), 1.99–0.81 (m, 6H). ¹³C NMR (100 MHz, DMSO) δ: 163.2, 157.9, 154.2, 143.3, 143.1, 133.0, 132.6, 129.4, 126.0, 119.1, 108.5, 61.9, 52.6, 49.0, 31.8, 31.6, 26.3, 23.4, 16.1. ESI-MS: *m/z* 565.5 [M + 1]⁺. C₂₈H₃₂N₆O₃S₂ (564.1977). HPLC purity: 95.37%.

4-((4-((4-Cyano-2,6-dimethylphenoxy)-7,8-dihydro-6H-thiopyrano[3,2-*d*]pyrimidin-2-yl)amino)piperidin-1-yl)methyl)benzamide (13f2). Recrystallized from EA/PE as a white solid, 74% yield. Mp: 261–263 °C. ¹H NMR (400 MHz, DMSO-*d*₆) δ: 7.91 (s, 1H), 7.81 (d, *J* = 8.1 Hz, 2H), 7.66 (s, 2H), 7.33 (d, *J* = 7.9 Hz, 2H), 7.30 (s, 1H), 6.86 (br, 1H), 3.43 (s, 2H), 3.08–2.94 (m, 2H), 2.69 (t, *J* = 6.2 Hz, 4H), 2.17–2.10 (m, 2H), 2.09 (s, 1H), 2.06 (s, 6H), 1.60 (s, 4H), 1.31 (s, 2H). ¹³C NMR (100 MHz, DMSO) δ: 168.2, 163.2, 158.0, 154.2, 142.6, 142.5, 133.4, 133.0, 132.6, 128.8, 127.8, 119.1, 108.5, 79.6, 62.1, 52.6, 31.8, 31.6, 31.1, 26.3, 23.4, 16.1. ESI-MS: *m/z* 529.5 [M + 1]⁺, 551.6 [M + 23]⁺. C₂₉H₃₂N₆O₂S (528.2307). HPLC purity: 96.74%.

3,5-Dimethyl-4-((2-((1-(4-(methylsulfonyl)benzyl)piperidin-4-yl)amino)-7,8-dihydro-6H-thiopyrano[3,2-*d*]pyrimidin-4-yl)oxy)benzimidazole (13f3). Recrystallized from EA/PE as a white solid, 66% yield. Mp: 265–267 °C. ¹H NMR (400 MHz, DMSO-*d*₆) δ: 7.87 (d, *J* = 8.3 Hz, 2H), 7.66 (s, 2H), 7.54 (d, *J* = 8.2 Hz, 2H), 6.89 (br, 1H), 3.50 (s, 2H), 3.20 (s, 3H), 3.10–2.95 (m, 2H), 2.69 (t, *J* = 6.2 Hz, 4H), 2.11 (m, 2H), 2.09 (s, 1H), 2.06 (s, 6H), 1.64 (s, 4H), 1.32 (s, 2H). ¹³C NMR (100 MHz, DMSO) δ: 163.2, 158.0, 157.9, 154.2, 145.4, 139.8, 133.0, 132.6, 129.7, 127.3, 119.1, 108.5, 61.8, 52.6, 48.6, 44.0, 31.8,

31.6, 26.3, 23.4, 16.1. ESI-MS: m/z 564.5 $[M + 1]^+$, 586.5 $[M + 23]^+$. $C_{29}H_{33}N_3O_3S_2$ (563.2025). HPLC purity: 96.93%.

3,5-Dimethyl-4-((2-((1-(4-nitrobenzyl)piperidin-4-yl)amino)-7,8-dihydro-6H-thiopyrano[3,2-d]pyrimidin-4-yl)oxy)-benzimidazole (13f4). Recrystallized from EA/PE as a white solid, 52% yield. Mp: 190–192 °C. 1H NMR (400 MHz, DMSO- d_6) δ : 8.18 (d, J = 8.7 Hz, 2H), 7.66 (s, 2H), 7.55 (d, J = 8.6 Hz, 2H), 6.88 (s, 1H), 3.53 (s, 2H), 3.11–2.92 (m, 2H), 2.69 (t, J = 6.2 Hz, 4H), 2.19–2.10 (m, 2H), 2.09 (s, 1H), 2.06 (s, 6H), 1.59 (s, 4H), 1.33 (s, 2H). ^{13}C NMR (100 MHz, DMSO) δ : 163.2, 157.9, 154.2, 147.5, 146.9, 133.0, 132.6, 130.0, 123.8, 119.1, 108.5, 61.6, 52.6, 31.8, 31.6, 31.1, 26.3, 23.4, 19.0, 16.1. ESI-MS: m/z 531.5 $[M + 1]^+$. $C_{28}H_{30}N_6O_3S$ (530.2100). HPLC purity: 99.57%.

3-((4-((4-(4-Cyano-2,6-dimethylphenoxy)-7,8-dihydro-6H-thiopyrano[3,2-d]pyrimidin-2-yl)amino)piperidin-1-yl)methyl)benzamide (13f5). Recrystallized from EA/PE as a white solid, 71% yield. Mp: 245–247 °C. 1H NMR (400 MHz, DMSO- d_6) δ : 7.95 (s, 1H), 7.76 (d, J = 11.6 Hz, 2H), 7.66 (s, 2H), 7.39 (d, J = 7.3 Hz, 2H), 7.33 (s, 1H), 6.86 (s, 1H), 3.43 (s, 2H), 3.02 (s, 2H), 2.77–2.58 (m, 4H), 2.19–2.09 (m, 2H), 2.09 (s, 1H), 2.06 (s, 6H), 1.63 (s, 4H), 1.32 (s, 2H). ^{13}C NMR (100 MHz, DMSO) δ : 168.4, 163.2, 157.9, 154.2, 139.2, 134.6, 133.0, 132.6, 132.0, 128.4, 126.4, 119.1, 108.5, 62.4, 52.6, 48.8, 31.8, 31.6, 31.1, 26.3, 23.4, 16.1. ESI-MS: m/z 529.4 $[M + 1]^+$. $C_{29}H_{32}N_6O_2S$ (528.2307). HPLC purity: 95.88%.

■ ASSOCIATED CONTENT

Supporting Information

The Supporting Information is available free of charge on the ACS Publications website at DOI: 10.1021/acs.jmedchem.8b01656.

Experimental procedures and characterizations of derivatives, in vitro assay of anti-HIV activities in TZM-bl cells, in vitro assay of anti-HIV activities in MT-4 cells, recombinant HIV-1 reverse transcriptase (RT) inhibitory assays, computational modeling, cytochrome P450 inhibition assay, plasma protein binding assay, pharmacokinetic methods, acute toxicity experiment, and assay procedures for hERG activity (PDF)

Molecular formula strings and some data (CSV)

■ AUTHOR INFORMATION

Corresponding Authors

*P.Z.: e-mail, zhanpeng1982@sdu.edu.cn; phone, 086-531-88382005.

*X.L.: e-mail, xinyongl@sdu.edu.cn; phone, 086-531-88380270.

ORCID

Dongwei Kang: 0000-0001-9232-953X

Francisco Javier Luque: 0000-0002-8049-3567

Jian Zhang: 0000-0002-5668-2974

Kuo-Hsiung Lee: 0000-0002-6562-0070

Peng Zhan: 0000-0002-9675-6026

Notes

The authors declare no competing financial interest.

The authors declare that all experimental work complied with the institutional guidelines on animal studies (care and use of laboratory animals).

■ ACKNOWLEDGMENTS

We gratefully acknowledge financial support from the Key Project of NSFC for International Cooperation (Grant 81420108027), the National Natural Science Foundation of China (NSFC Grants 81273354 and 81573347), Young Scholars Program of Shandong University (YSPSDU Grant 2016WLJH32), Key Research and Development Project of

Shandong Province (Grant 2017CXGC1401), KU Leuven (Grant GOA 10/014), and National Institutes of Health (Grant AI033066). We acknowledge the Spanish Ministerio de Economía y Competitividad (Grant SAF2017-88107-R) and the Generalitat de Catalunya (Grant 2017SGR1746) for financial support and the Barcelona Supercomputing Center (Grant BCV-2018-2-0006) and Consorci de Serveis Universitaris de Catalunya (Molecular Recognition) for computational resources. We acknowledge Prof. Thomas A. Steitz and express our gratitude and remembrance to him.

■ ABBREVIATIONS USED

AIDS, acquired immune deficiency syndrome; CC_{50} , 50% cytotoxicity concentration; DAPY, dihydropyrimidine; DLV, delavirdine; EFV, efavirenz; ETV, etravirine; EC_{50} , effective concentration causing 50% inhibition of viral cytopathogenicity; HAART, highly active antiretroviral therapy; HIV, human immunodeficiency virus; hERG, human ether-à-go-go related gene; MD, molecular dynamics; NNIBP, NNRTI binding pocket; NNRTI, non-nucleoside reverse transcriptase inhibitor; NRTI, nucleoside reverse transcriptase inhibitor; NVP, nevirapine; RF, fold-resistance; RMSD, root-mean-square displacement; RMSF, root-mean-square fluctuation; RPV, rilpivirine; RT, reverse transcriptase; SAR, structure–activity relationship; SI, selectivity index; WT, wild-type

■ REFERENCES

- (1) Shattock, R. J.; Warren, M.; McCormack, S.; Hankins, C. A. AIDS. Turning the tide against HIV. *Science* **2011**, *333*, 42–43.
- (2) Bec, G.; Meyer, B.; Gerard, M. A.; Steger, J.; Fauster, K.; Wolff, P.; Burnouf, D.; Micura, R.; Dumas, P.; Ennifar, E. Thermodynamics of HIV-1 reverse transcriptase in action elucidates the mechanism of action of non-nucleoside inhibitors. *J. Am. Chem. Soc.* **2013**, *135*, 9743–9752.
- (3) Zhan, P.; Chen, X.; Li, D.; Fang, Z.; De Clercq, E.; Liu, X. HIV-1 NNRTIs: structural diversity, pharmacophore similarity, and implications for drug design. *Med. Res. Rev.* **2013**, *33* (Suppl. 1), E1–E72.
- (4) Zhan, P.; Pannecouque, C.; De Clercq, E.; Liu, X. Anti-HIV drug discovery and development: current innovations and future trends. *J. Med. Chem.* **2016**, *59*, 2849–2878.
- (5) Li, D.; Zhan, P.; De Clercq, E.; Liu, X. Strategies for the design of HIV-1 non-nucleoside reverse transcriptase inhibitors: lessons from the development of seven representative paradigms. *J. Med. Chem.* **2012**, *55*, 3595–3613.
- (6) Johnson, J. A.; Li, J. F.; Morris, L.; Martinson, N.; Gray, G.; McIntyre, J.; Heneine, W. Emergence of drug-resistant HIV-1 after intrapartum administration of single-dose nevirapine is substantially underestimated. *J. Infect. Dis.* **2005**, *192*, 16–23.
- (7) Johnson, V. A.; Brun-Vezinet, F.; Clotet, B.; Conway, B.; D'Aquila, R. T.; Demeter, L. M.; Kuritzkes, D. R.; Pillay, D.; Schapiro, J. M.; Telenti, A.; Richman, D. D. Drug resistance mutations in HIV-1. *Top. HIV Med.* **2003**, *11*, 215–221.
- (8) Lehman, D. A.; Wamalwa, D. C.; McCoy, C. O.; Matsen, F. A.; Langat, A.; Chohan, B. H.; Benki-Nugent, S.; Custers-Allen, R.; Bushnan, F. D.; John-Stewart, G. C.; Overbaugh, J. Low-frequency nevirapine resistance at multiple sites may predict treatment failure in infants on nevirapine-based treatment. *JAIDS, J. Acquired Immune Defic. Syndr.* **2012**, *60*, 225–233.
- (9) Wainberg, M. A.; Zaharatos, G. J.; Brenner, B. G. Development of antiretroviral drug resistance. *N. Engl. J. Med.* **2011**, *365*, 637–646.
- (10) Beyrer, C.; Pozniak, A. HIV drug resistance - an emerging threat to epidemic control. *N. Engl. J. Med.* **2017**, *377*, 1605–1607.
- (11) Kang, D.; Fang, Z.; Li, Z.; Huang, B.; Zhang, H.; Lu, X.; Xu, H.; Zhou, Z.; Ding, X.; Daelemans, D.; De Clercq, E.; Pannecouque, C.; Zhan, P.; Liu, X. Design, synthesis, and evaluation of thiophene[3,2-d]pyrimidine derivatives as HIV-1 non-nucleoside reverse transcriptase

inhibitors with significantly improved drug resistance profiles. *J. Med. Chem.* **2016**, *59*, 7991–8007.

(12) Kang, D.; Fang, Z.; Huang, B.; Lu, X.; Zhang, H.; Xu, H.; Huo, Z.; Zhou, Z.; Yu, Z.; Meng, Q.; Wu, G.; Ding, X.; Tian, Y.; Daelemans, D.; De Clercq, E.; Pannecouque, C.; Zhan, P.; Liu, X. Structure-based optimization of thiophene[3,2-*d*]pyrimidine derivatives as potent HIV-1 non-nucleoside reverse transcriptase inhibitors with improved potency against resistance-associated variants. *J. Med. Chem.* **2017**, *60*, 4424–4443.

(13) Yang, Y.; Kang, D.; Nguyen, L. A.; Smithline, Z. B.; Pannecouque, C.; Zhan, P.; Liu, X.; Steitz, T. A. Structural basis for potent and broad inhibition of HIV-1 RT by thiophene[3,2-*d*]pyrimidine non-nucleoside inhibitors. *eLife* **2018**, *7*, No. e36340.

(14) Lee, W. G.; Gallardo-Macias, R.; Frey, K. M.; Spasov, K. A.; Bollini, M.; Anderson, K. S.; Jorgensen, W. L. Picomolar inhibitors of HIV reverse transcriptase featuring bicyclic replacement of a cyanovinylphenyl group. *J. Am. Chem. Soc.* **2013**, *135*, 16705–16713.

(15) Kang, D.; Huo, Z.; Wu, G.; Xu, J.; Zhan, P.; Liu, X. Novel fused pyrimidine and isoquinoline derivatives as potent HIV-1 NNRTIs: a patent evaluation of WO2016105532A1, WO2016105534A1 and WO2016105564A1. *Expert Opin. Ther. Pat.* **2017**, *27*, 383–391.

(16) Ishikawa, M.; Hashimoto, Y. Improvement in aqueous solubility in small molecule drug discovery programs by disruption of molecular planarity and symmetry. *J. Med. Chem.* **2011**, *54*, 1539–1554.

(17) Takeuchi, T.; Oishi, S.; Kaneda, M.; Ohno, H.; Nakamura, S.; Nakanishi, I.; Yamane, M.; Sawada, J.-i.; Asai, A.; Fujii, N. Kinesin spindle protein inhibitors with diaryl amine scaffolds: crystal packing analysis for improved aqueous solubility. *ACS Med. Chem. Lett.* **2014**, *5*, 566–571.

(18) Carroll, S. S.; Olsen, D. B.; Bennett, C. D.; Gotlib, L.; Graham, D. J.; Condra, J. H.; Stern, A. M.; Shafer, J. A.; Kuo, L. C. Inhibition of HIV-1 reverse transcriptase by pyridinone derivatives. Potency, binding characteristics, and effect of template sequence. *J. Biol. Chem.* **1993**, *268*, 276–281.

(19) Liu, N.; Wei, L.; Huang, L.; Yu, F.; Zheng, W.; Qin, B.; Zhu, D. Q.; Morris-Natschke, S. L.; Jiang, S.; Chen, C. H.; Lee, K. H.; Xie, L. Novel HIV-1 non-nucleoside reverse transcriptase inhibitor agents: optimization of diarylanilines with high potency against wild-type and rilpivirine-resistant E138K mutant virus. *J. Med. Chem.* **2016**, *59*, 3689–3704.

(20) Freeman-Cook, K. D.; Hoffman, R. L.; Johnson, T. W. Lipophilic efficiency: the most important efficiency metric in medicinal chemistry. *Future Med. Chem.* **2013**, *5*, 113–115.

(21) Tarcsay, A.; Nyiri, K.; Keseru, G. M. Impact of lipophilic efficiency on compound quality. *J. Med. Chem.* **2012**, *55*, 1252–1260.